The Astrophysical Journal, 675:1025–1040, 2008 March 10

THE EVOLUTION OF AGN HOST GALAXIES: FROM BLUE TO RED AND THE INFLUENCE OF LARGE-SCALE STRUCTURES

J. D. Silverman,[1] V. Mainieri,[1,2] B. D. Lehmer,[3] D. M. Alexander,[4] F. E. Bauer,[5] J. Bergeron,[6,7] W. N. Brandt,[3] R. Gilli,[8] G. Hasinger,[1] D. P. Schneider,[3] P. Tozzi,[9] C. Vignali,[10] A. M. Koekemoer,[11] T. Miyaji,[11] P. Popesso,[2,7] P. Rosati,[2,7] and G. Szokoly[1]

Received 2007 May 22; accepted 2007 November 19

ABSTRACT

We present an analysis of 109 moderate-luminosity ($41.9 \leq \log L_{0.5-8.0\,\mathrm{keV}} \leq 43.7$) AGNs in the Extended *Chandra* Deep Field-South survey, which is drawn from 5549 galaxies from the COMBO-17 and GEMS surveys having $0.4 \leq z \leq 1.1$. These obscured or optically weak AGNs facilitate the study of their host galaxies since the AGNs provide an insubstantial amount of contamination to the galaxy light. We find that the color distribution of AGN host galaxies is highly dependent on (1) the strong color-evolution of luminous ($M_V < -20.7$) galaxies, and (2) the influence of $\sim$10 Mpc scale structures. When excluding galaxies within the redshift range $0.63 \leq z \leq 0.76$, a regime dominated by sources in large-scale structures at $z = 0.67$ and $z = 0.73$, we observe a bimodality in the host galaxy colors. Galaxies hosting AGNs at $z \gtrsim 0.8$ preferentially have bluer (rest-frame $U - V < 0.7$) colors than their $z \lesssim 0.6$ counterparts (many of which fall along the red sequence). The fraction of galaxies hosting AGNs peaks in the "green valley" ($0.5 < U - V < 1.0$); this is primarily due to enhanced AGN activity in the redshift interval $0.63 \leq z \leq 0.76$. The AGN fraction in this redshift and color interval is 12.8% (compared to its "field" value of 7.8%) and reaches a maximum of 14.8% at $U - V \sim 0.8$. We further find that blue, bulge-dominated (Sérsic index $n > 2.5$) galaxies have the highest fraction of AGN (21%) in our sample. We explore the scenario that the evolution of AGN hosts is driven by galaxy mergers and illustrate that an accurate assessment requires a larger area survey since only three hosts may be undergoing a merger with timescales $\lesssim$1 Gyr following a starburst phase.

Subject headings: galaxies: active — galaxies: evolution — large-scale structure of universe — quasars: general — X-rays: galaxies

1. INTRODUCTION

There has been remarkable evidence found in the last few years that the evolution of supermassive black holes (SMBHs) and galaxies are inextricably linked. For instance, ultraluminous infrared and submillimeter galaxies (Alexander et al. 2005), with prodigious rates of star formation, show a high fraction of AGN activity. Current models of galaxy evolution (e.g., Di Matteo et al. 2005; Hopkins et al. 2005; Springel et al. 2005b) demonstrate that merger-driven feedback from an AGN may quench star formation, contributing to the order-of-magnitude decline in the cosmic star formation rate (SFR) and QSO emissivity (Boyle & Terlevich 1998; Franceschini et al. 1999; Merloni et al. 2004) observed between $z \sim 1$ and the present day. This self-regulated growth may then establish the correlation between the mass of the central black hole and the stellar velocity dispersion of the host bulge (Ferrarese & Merritt 2000; Gebhardt et al. 2000; Tremaine et al. 2002).

A clear imprint of this scenario may be evident in the properties (e.g., color and morphology) of the host galaxies of AGNs caught at early epochs in their evolution. Much effort has been undertaken to detect the hosts of nearby bright QSOs (e.g., Bahcall et al. 1997; Jahnke et al. 2004a; McLure et al. 2004), although this endeavor remains challenging. Surveys of obscured AGNs, selected through various means (e.g., optical emission lines, X-rays, or reradiated infrared emission), offer the potential to measure cleanly the ages, stellar populations, and SFRs of these host galaxies (e.g., Sturm et al. 2006). Kauffmann et al. (2003) clearly show that the hosts of narrow emission line AGN ($z < 0.3$) in the Sloan Digital Sky Survey (SDSS) are predominately massive, early-type galaxies and that those with the most-luminous AGNs have significant star formation with younger mean stellar ages. Deep X-ray surveys (see Brandt & Hasinger 2005 for a review) are generating significant samples of obscured AGNs closer to the peak ($z \sim 1$) of the global star-formation and merger rate of galaxies (Hopkins et al. 2006a; Kartaltepe et al. 2007). Recently, Nandra et al. (2007) have shown that the host galaxies of moderate-luminosity AGNs with $0.6 < z < 1.4$, found in the Extended Groth Strip, have a broad range of optical colors that span the same region of the color-magnitude relation as luminous ($M_B < -20.5$) galaxies. The prevalence of AGN host galaxies within the region separating the blue and red galaxy populations may lend support for the importance of AGN feedback since this location is thought to represent a transitional phase in the evolution of galaxies.

[1] Max-Planck-Institut für extraterrestrische Physik, D-84571 Garching, Germany.
[2] European Southern Observatory, Karl-Schwarzschild-Strasse 2, Garching, D-85748, Germany.
[3] Department of Astronomy and Astrophysics, 525 Davey Lab, The Pennsylvania State University, University Park, PA 16802.
[4] Department of Physics, University of Durham, South Road, Durham, DH1 3LE, UK.
[5] Columbia Astrophysics Laboratory, Columbia University, Pupin Labortories, 550 West 120th Street, Room 1418, New York, NY 10027.
[6] Institut d'Astrophysique de Paris, 98bis Boulevard, F-75014 Paris, France.
[7] Based on observations made at the European Southern Observatory, Paranal, Chile (ESO programs 170.A-0788, 171.A-3045, 072.A-0139).
[8] Istituto Nazionale di Astrofisica (INAF)-Osservatorio Astronomico di Bologna, Via Ranzani 1, 40127 Bologna, Italy.
[9] INAF–Osservatorio Astronomico di Trieste, via G. B. Tiepolo 11, 34131 Trieste, Italy.
[10] Dipartimento di Astronomia, Universitá degli Studi di Bologna, Via Ranzani 1, 40127 Bologna, Italy.
[11] Space Telescope Science Institute, 3700 San Martin Drive, Baltimore, MD 21218.
[12] Department of Physics, Carnegie Mellon University, Pittsburgh, PA 15213.

It is of much interest to constrain observationally whether environment plays a significant role in the growth of SMBHs, as expected by merger-driven accretion models. Observational support for the importance of mergers is mainly based on circumstantial evidence: (1) AGN predominately reside in massive, early-type galaxies (e.g., Kauffmann et al. 2003), of which many are massive ellipticals, well thought to be the end-product of a major-merger between gas-rich disk galaxies, (2) ultraluminous infrared galaxies, which are morphologically disturbed in almost all cases, have a high fraction ($\sim$50%) of AGN activity and large molecular gas concentrations in their nuclei (see Sanders & Mirabel 1996). Studies of low-redshift ($z < 0.3$) AGNs from the SDSS indicate that the fraction of galaxies harboring AGN is independent of environment (e.g., Miller et al. 2003) even in the cores of massive clusters. For the most-luminous narrow-line AGNs in the SDSS (Kauffmann et al. 2004), an AGN-fraction–density relation has been shown to exist analogous to the SFR-density relation with a higher AGN fraction in low-density (i.e., "field") environments. Both studies provide evidence counter to the expectation that SMBH accretion is induced by galaxy mergers. Hard X-ray-selected surveys, most effective at identifying obscured accretion at higher redshifts, also present disparate views on the relationship between AGN activity and their environments. Georgakakis et al. (2007) present preliminary results that demonstrate that X-ray-selected AGN at $z \sim 1$ "avoid" underdense regions and those with blue ($U - V \lesssim 1$) hosts are found in denser environments, hinting at a connection to star formation. On the contrary, Grogin et al. (2005) find that AGN in the *Chandra* Deep Fields show no evidence for an environmental dependency based on similar AGN host morphologies and near-neighbor counts to the nonactive galaxy population. The AGN fraction in clusters (Martini et al. 2006, 2007), although higher than previously determined (Dressler & Gunn 1983), is not significantly different than that in the "field"; a different picture may emerge at higher redshifts since Eastman et al. (2007) find significant evolution of the AGN fraction in clusters at $z \sim 0.6$. There is also evidence that larger scale ($\gtrsim$0.1 Mpc) structures may play an important role in AGN fueling. Li et al. (2006) have measured the cross-correlation function of narrow-line AGNs in the SDSS with a well-controlled sample of nonactive galaxies, and find that AGNs are primarily not associated with major mergers of galaxies, and preferentially lie within the densest peaks of the underlying dark-matter distribution. Gilli et al. (2003) find that 30% of the X-ray-selected AGNs in the 1 Ms CDF-S are located within narrow redshift slices at $z = 0.67$ and $z = 0.73$ and spread across the full *Chandra* field-of-view ($17' \times 17'$), which corresponds to a physical scale of 7.3 Mpc at $z = 0.7$. Similar structures are evident in the CDF-N (Barger et al. 2003) that may indicate the importance of large-scale ($\sim$10 Mpc) structures to trigger mass accretion onto SMBHs.

The Extended *Chandra* Deep Field-South (E-CDF-S) is an ideal survey field to use for investigating the properties of galaxies harboring AGNs and the role of environment due to its remarkable multiwavelength coverage. We have completed a 1 Ms *Chandra* Legacy program (PI: W. N. Brandt; Lehmer et al. 2005) that covers a wide area (0.33 deg^2, 3 times area of the CDF-S) at the depths required to detect moderate-luminosity ($L_X \sim 10^{43}$ ergs s^{-1}) AGNs, including those with significant obscuration, out to the quasar epoch ($z \sim 2.5$). The optical coverage of the E-CDF-S is extensive, providing large galaxy samples with a wealth of multiwavelength data. For example, the COMBO-17 survey (Wolf et al. 2004) has imaged the field with 12 narrowband and five broadband optical filters, thus providing magnitudes, accurate photometric redshifts ($\sigma_z \approx 0.03$) and galaxy spectral energy distribution types that further aid in the identification of the X-ray source counterparts. Optical morphological information is available from the *Hubble Space Telescope* (*HST*) Advanced Camera for Surveys (ACS) observations via the GEMS (Rix et al. 2004; Häussler et al. 2007), GOODS (Giavalisco et al. 2004) and the *HST* Ultra Deep field (UDF; Beckwith et al. 2006) projects. Over 1000 spectroscopic redshifts are available via the CDF-S (Szokoly et al. 2004), VVDS (Le Fevre et al. 2004), K20 (Mignoli et al. 2005), and GOODS (Vanzella et al. 2005, 2006) surveys.

In this paper we investigate the location of moderate-luminosity AGNs, in the E-CDF-S, on the color-magnitude diagram and their relation to the underlying galaxy population using our current catalog of X-ray-selected AGNs with either spectroscopic or photometric redshifts. The E-CDF-S contains two prominent redshift spikes (Gilli et al. 2003) enabling us to determine the influence of $\sim$10 Mpc structures on the overall color-magnitude distribution. We discuss how our results fit in with the morphological properties of the sample and the impact on galaxy evolution models that incorporate AGN feedback to quench star formation effectively. Throughout this work, we assume $H_0 = 70$ km s^{-1} Mpc^{-1}, $\Omega_\Lambda = 0.7$, and $\Omega_M = 0.3$.

2. DATA

We select a parent sample of galaxies in the E-CDF-S using published catalogs from the COMBO-17 and GEMS surveys. The *Chandra* observations, covering the equivalent sky area, enable identification of those galaxies that harbor moderate-luminosity AGNs in a manner that is least biased against obscuration. Follow-up optical spectroscopy of these X-ray sources with the VLT facilitates the identification of AGNs. As detailed below, our selection is tuned to generate a sample of galaxies hosting AGNs for which the optical emission is dominated by the host galaxy; thus no further removal of AGN light (i.e., cleaning) is required for this study. By restricting ourselves to an initial optically selected sample of galaxies, we aim to measure the fraction of galaxies harboring AGNs as a function of their intrinsic properties.

2.1. *Parent Galaxy Population*

COMBO-17 provides a highly complete sample of galaxies over the full E-CDF-S (Wolf et al. 2004) with well-known intrinsic properties (i.e., magnitudes and colors). The survey provides reliable object classifications (e.g., galaxy, QSO, star) and photometric redshifts by fitting synthetic template optical spectra to the observed magnitudes over a broad wavelength range (3500–9300 Å). The source catalog contains 8565 objects with aperture magnitudes $R_{ap} \leq 24$, a limit at which there are photometric redshift errors of $\delta_z/(1+z) < 0.1$. This magnitude limit ensures that our sample is representative of galaxies of all colors with $M_V \lesssim -21$ and $z < 1$, a limit that will be shown to be relevant for this study. Full details including source detection, photometry, object classification, and redshift estimation can be found in Wolf et al. (2004). Morphological information is provided by *HST* ACS imaging of the field in both the F606W and F850LP filters (hereafter referred to V_{606} and z_{850}, respectively) from GEMS. Here, we use the Sérsic indices (n) given in Häussler et al. (2007) to discriminate between bulge and disk-dominated galaxies.

We select a sample of 5549 galaxies with photometric redshifts of $0.4 \leq z \leq 1.1$ from the GEMS z_{850}-band selected catalog of Caldwell et al. (2008) that has been cross-referenced to objects in COMBO-17 ($R_{ap} \leq 24$). This ensures that the sample can be used for morphological studies and allows an upper limit to be placed on the optical contribution from each AGN to the color of its host galaxy. The sample includes only those objects that are classified as a "galaxy" and excludes those identified as a

"QSO." This selection effectively avoids the presence of luminous type 1 AGNs that severely dilute the emission from their host galaxies. The lower redshift limit is set to 0.4 because this volume within the E-CDF-S is too small at lower redshifts to generate statistically useful samples of luminous ($M_V \lesssim -21$) galaxies and hence those with AGNs. Only two AGNs have been unambigously identified at $z < 0.4$ that have $L_X \sim 10^{42}$ ergs s^{-1}. The redshift cutoff at 1.1 is the limit for which COMBO-17 no longer provides accurate source classification, and redshifts are susceptible to large uncertainties. We primarily use the rest-frame optical magnitudes (M_U, M_V; Vega magnitudes), publicly available from COMBO-17 (Wolf et al. 2004), derived from synthetic galaxy templates to measure intrinsic luminosity and color. To compare with theoretical models (§ 6.4), we utilize the rest-frame u and r (SDSS) also provided by COMBO-17. The errors (1 σ; Wolf et al. 2004) on rest-frame magnitudes are typically 0.11 (M_U) and 0.15 mag (M_V). Throughout this work, a representative error (1 σ) on color ($U - V$) is determined to be 0.19 from the quadrature of the errors of the individual rest-frame magnitudes; this is most likely an overestimate since these magnitude errors are correlated. Bell et al. (2004) report a typical error on $U - V$ to be $\sim$0.1 mag.

2.2. *AGN Identification*

We compile a sample of AGNs, based on their high X-ray luminosities, in the E-CDF-S by matching the 762 *Chandra* point sources given in Lehmer et al. (2005) to the available optical and near-infrared catalogs. We do not consider here the fainter X-ray sources solely detected in the 1 Ms CDF-S to maintain a fairly uniform sensitivity across the entire E-CDF-S. Redshifts are available for 362 (48%) of the X-ray sources through either spectroscopic or photometric techniques. We significantly improve on the 97 spectroscopic redshifts available in the literature (Szokoly et al. 2004; Le Fevre et al. 2004; Mignoli et al. 2005; Vanzella et al. 2005, 2006) with 95 additional redshifts acquired by observations with VIMOS (Le Fevre et al. 2003) on the VLT through the ESO programs 072.A-0139 (PI: J. Bergeron; 65 redshifts; J. D. Silverman et al. 2008, in preparation) and 171.A-3045 (GOODS; PI: C. Cesarski; 30 redshifts; P. Popesso et al., in preparation). Our VIMOS observations are unique since we have acquired spectra over a wide wavelength range (3600–9500 Å) for many targets by observing with both the LRblue and MRred grisms. With integration times reaching 5 hr, we are able to detect faint spectral features (e.g., [O II], Mg II, Fe II) in many of the host galaxies of obscured or optically faint AGNs that enable a redshift measurement. A detailed discussion of the VIMOS observations will be provided in a subsequent paper (Silverman et al. 2008, in preparation). The X-ray luminosity of each AGN is determined from their observed broadband (0.5–8.0 keV) flux, given in Lehmer et al. (2005) with a k-correction based on a power-law spectrum (photon index $\Gamma = 1.9$) and no correction for intrinsic absorption. Here, we restrict the luminosity range to $41.9 \leq \log L_{0.5-8.0\,\mathrm{keV}} \leq 43.7$. The lower luminosity limit is chosen to provide a robust sample free of any galaxies having significant X-ray binary or diffuse X-ray emission; luminous starburst galaxies in the *Chandra* Deep Fields are typically a factor of $\sim$10 fainter (see Fig. 4 of Bauer et al. 2002). We also minimize potential luminosity-dependent effects since lower luminosity AGNs would only be detected over a small fraction of the redshift range ($z = 0.4$–1.1) considered here. The *Chandra* observations of the E-CDF-S are capable of detecting AGNs at this lower luminosity limit up to $z \sim 0.85$. Our upper limit is motivated by Silverman et al. (2005), who show that the optical emission, associated with X-ray-selected AGNs at $\log \nu l_\nu < 43.3$ at $E = 2$ keV, is primarily due to their host galaxy since there is a strong departure of these AGNs from the known l_{opt}-l_X relation for more luminous X-ray-selected AGNs. We convert this limit to a broadband (0.5–8.0 keV) X-ray luminosity of $10^{43.7}$ ergs s^{-1} assuming the same spectrum as given above. Furthermore, our adopted upper limit is similar to that of Nandra et al. (2007), who demonstrate that the host galaxies of moderate-luminosity AGNs, at X-ray fluxes equivalent to those detected in the E-CDF-S, contribute the majority of the total optical emission. As detailed below, we have measured upper limits to the AGN contribution, using the *HST* ACS imaging of the field, and show that the optical emission, for the majority of our sample, is dominated by the host galaxy. Optical spectra provide a final check on the AGN contribution with most sources clearly lacking any faint broad emission lines or a rising blue continuum.

A cross-correlation of the X-ray and optical catalogs has indicated that 109 of the 5549 galaxies have AGNs with $L_X \approx 10^{41.9}$–$10^{43.7}$ erg s^{-1}. Of these, spectroscopic redshifts were available for 54 of these sources, 16 (seven at $z > 1$) of which were from our VIMOS observations. Rest-frame magnitudes for 12 galaxies were rederived (C. Wolf 2007, private communication) using COMBO-17 tools since their spectroscopic redshifts differed substantially from their photometric redshifts ($\Delta z > 0.1$) that rendered their rest-frame optical magnitudes published by COMBO-17 as inaccurate. This is not surprising since seven of them have spectroscopic redshifts of $z \sim 1$, a regime where photometric redshifts for galaxies in COMBO-17 show a higher dispersion (see Fig. 6 of Wolf et al. 2004), and lack strong continuum features (e.g., 4000 Å break) most useful for adequate photometric redshift estimates. Our AGN sample is primarily radio-quiet since only nine have a radio-loudness (R) greater than 10 ($R \equiv L_{6\,\mathrm{cm}}/L_{4400\,\text{Å}}$) based on 20 cm VLA detections (P. Tozzi et al. in preparation) that reach a flux limit of 8.5 μJy, optical emission attributed to the AGNs (25%; see the following section) based on our R-band optical magnitudes, and spectral indices ($L_\nu \propto \nu^{-\gamma}$; $\gamma_{\mathrm{radio}} = 0.8$, $\gamma_{\mathrm{opt}} = 0.5$). We refer the reader to Rovilos et al. (2007) for further details on the radio properties of X-ray-selected AGNs in the E-CDF-S. We further note that an additional 31 AGNs have redshifts and luminosities within our range of interest although fell out of the sample due to their faint optical magnitudes ($R_{\mathrm{ap}} > 24$). Our final sample of 109 AGNs allows us to compare the properties of their host galaxies to the underlying galaxy population.

2.3. *AGN Contribution to Host-Galaxy Emission*

We are confident that the optical emission, from these 109 galaxies hosting AGNs, is dominated by star light and not strongly influenced by the AGNs based on the following arguments. In Figure 1 we show that there is no correlation between X-ray luminosity and either rest-frame magnitude (M_V; Pearson correlation coefficient $r = -0.036$) or color ($U - V$, $r = -0.233$). This is consistent with the results of Nandra et al. (2007), who show that only a weak correlation exists for X-ray sources at similar low X-ray and optical fluxes. The lack of any correlation in our sample is due to the fact that we deliberately excluded the luminous ($\log L_X \gtrsim 44$) AGNs and any objects classified by COMBO-17 as a "QSO."

We determine conservative upper limits on the AGN contribution to the total (galaxy+AGN) light using the *HST* ACS V_{606}- and z_{850}-band images provided by GEMS. These images, available from MAST (Multimission Archive at Space Telescope), have been through the `mark1` processing as described in Caldwell et al. (2008) and are rescaled to 0.03″ pixel^{-1}. A few AGNs are not included in our analysis due to their proximity to the ACS field edge.

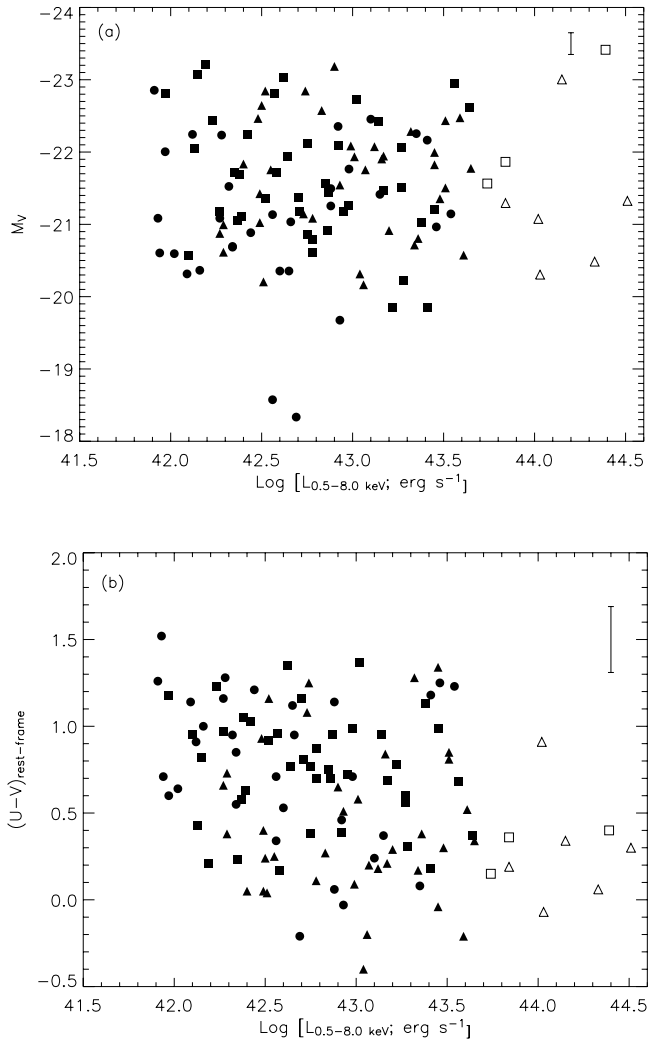

FIG. 1.—(*a*) Rest-frame absolute magnitude (M_V) and (*b*) optical color ($U - V$) as a function of X-ray luminosity for our sample of 109 AGNs (*filled symbols*). The type of marker denotes AGNs within three separate redshift intervals ($z = 0.4–0.63$, *circles*; $z = 0.63–0.76$, *squares*; $z = 0.76–1.1$, *triangles*). Open symbols show higher luminosity AGNs not included in our sample. A typical error bar of size $\pm 1\ \sigma$ is placed in the upper right corner in both panels.

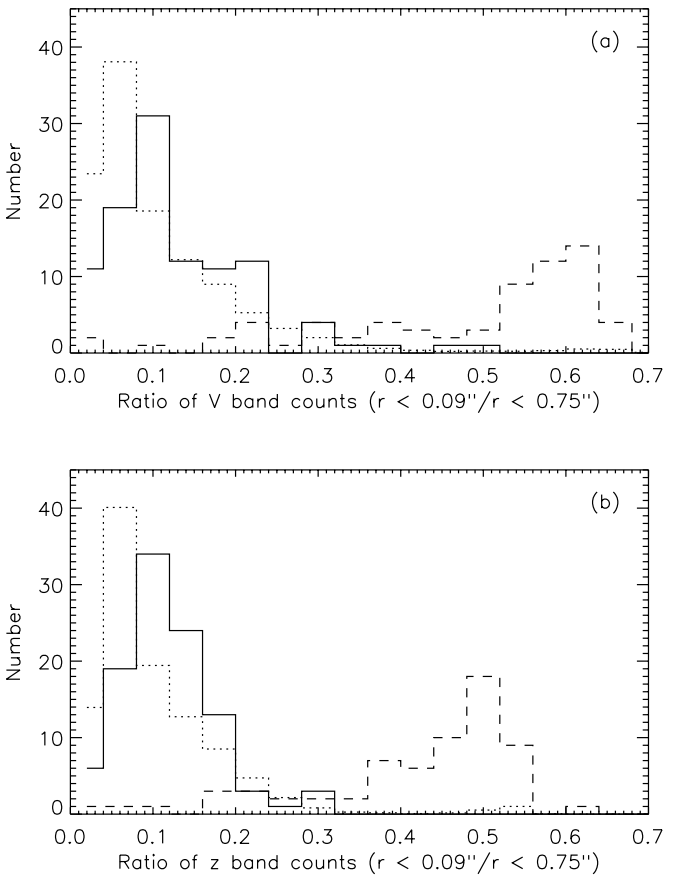

FIG. 2.—AGN contribution to the total (AGN+galaxy) light. The abscissa is the ratio of source counts in *HST* ACS images between a circular aperture of radius 0.09″ and 0.75″. In panel *a* the V_{606}-band count-ratio distribution is shown for 104 AGN (*solid histogram*), 5521 galaxies (*dotted histogram*), and 67 (*dashed histogram*) optically selected QSOs from COMBO-17. In panel *b* the same is shown for the z_{850}-band (103 AGN, 5513 galaxies, 66 QSOs). QSOs from COMBO-17 illustrate the typical count ratios for unresolved point sources. The galaxy number distribution in both panels has been scaled down to match the numbers of AGN host galaxies. The majority of the AGN host galaxies have $\gtrsim$80% of their total optical emission (in both the V_{606} and z_{850} bands) outside the circular aperture of radius 0.09″ and have count ratios similar to the non-AGN galaxy population.

Extended optical emission is clearly evident for all 109 galaxies hosting AGNs. Optical counts are measured without subtracting the background in circular apertures of two different sizes positioned at the centroid of the optical emission: (1) a small aperture with a radius of 3 pixels (0.09″) that contains 50% of the flux from an unresolved point source (see Jahnke et al. 2004b) and corresponds to a physical scale of 0.48 ($z = 0.4$) to 0.74 ($z = 1.1$) kpc, and (2) a larger aperture with a radius of 25 pixels (0.75″; covering a physical scale of 4.03–6.13 kpc). The size of the larger aperture is set to that implemented for flux extraction by COMBO-17 (Wolf et al. 2004). The counts within the small aperture provide a firm upper limit to the AGNs contribution since we make no attempt to remove emission of stellar origin. For comparison, we measure counts in equivalent regions for the entire sample of 5549 galaxies and 67 QSOs, which were identified by COMBO-17 and are not included in our parent galaxy sample.

The number distribution of the AGN host galaxies as a function of the ratio of counts between these two apertures is shown in Figure 2 for both the V_{606}-band (Fig. 2*a*) and z_{850}-band (Fig. 2*b*). Based on the V_{606}-band measurements, the mean ratio of counts of our AGN sample (*solid histogram*) is 0.14, and 81% of them have a ratio less than 0.2. The distribution is similar to that of the galaxies (*dotted histogram*), although shifted slightly by 0.04 (the difference of their median values), most likely due to the presence of optically faint AGNs. The host galaxy distribution is noticeably offset from that of the optically selected QSOs, identified by spectral template fitting with no preference for pointlike sources (Wolf et al. 2004), that have a mean ratio of 0.48, and 60% of them have a ratio greater than 0.5, most likely indicative of unresolved point sources. A number of low count ratio QSOs are evident due to the fact that COMBO-17 can recognize lower luminosity Seyfert 1 galaxies as QSOs if strong AGN features are present. Similar results are found for the z_{850}-band measurements, which suggests that color gradients are dominated by the host galaxies and not the underlying AGNs. Since our sample contains a large fraction of obscured AGNs, there is a slightly larger contribution from AGN emission in the z_{850} band compared to the V_{606} band, whereas the opposite is true for the quasars.

The maximum amount that an AGN could shift its host-galaxy rest-frame $U - V$ color blueward is estimated. We assume that an AGN contributes all the flux in the small ($r = 0.09''$) aperture, the count ratio as detailed above is 0.2, and the background signal is negligible. This corresponds to an AGN contributing an

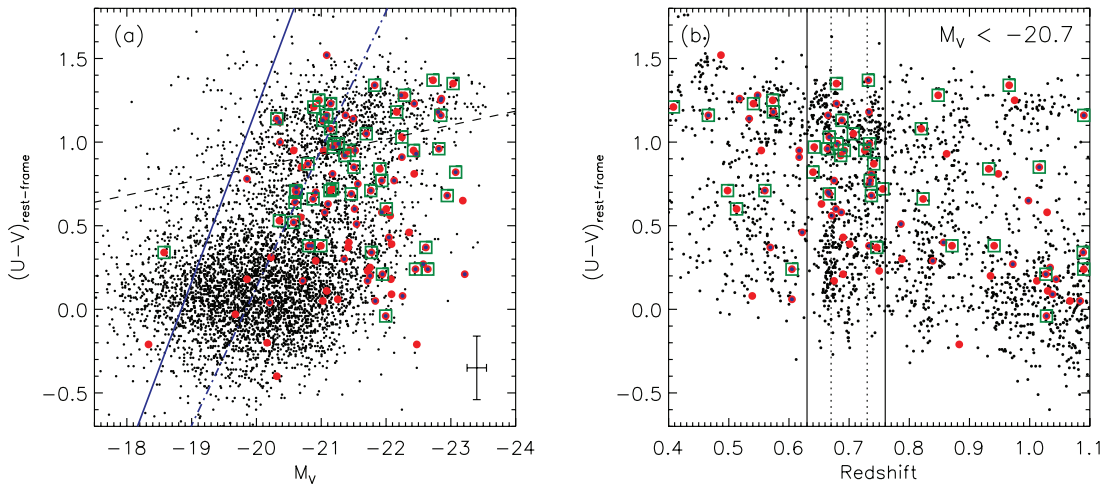

FIG. 3.—(*a*) Rest-frame optical color ($U - V$) as a function of rest-frame absolute magnitude (M_V) for 109 galaxies hosting AGNs compared to their parent sample of 5549 galaxies with $0.4 \leq z \leq 1.1$. Galaxies in the parent sample are marked with small black filled circles; those hosting X-ray-selected AGNs are highlighted by large red circles. The slanted blue lines denote the approximate limits for galaxies with $R_{ap} \leq 24$ at $z = 0.8$ (*solid histogram*) and $z = 1$ (*dash-dotted histogram*). The division between red and blue galaxies implemented by Bell et al. (2004) is shown by the dashed line. AGN hosts classified as bulge-dominated (Sérsic index 2.5–8) galaxies by the *HST* ACS morphology (Häussler et al. 2007) are marked with blue filled circles at the centers of the red circles. AGNs with X-ray hardness ratios larger than 0.2 (see § 6.4) are marked by open green squares in both panels. The typical error ($\pm 1\ \sigma$) bar is shown in the bottom right corner. (*b*) Rest-frame $U - V$ color versus redshift for the 2044 most luminous ($M_V < -20.7$) galaxies. The vertical solid lines denote the redshift interval $0.63 \leq z \leq 0.76$ with the dotted lines marking the redshift spikes at $z = 0.67$ and $z = 0.73$. In this panel only, smaller blue dots mark the AGNs with spectroscopic redshifts.

additional amount of flux equal to 0.25 times the total host galaxy flux. We further consider an AGN to add flux to the *U*-band only. While rest-frame UV emission is substantially diminished at $\lambda < 4000$ Å for a typical galaxy, broad-line AGN (Vanden Berk et al. 2006; Gavignaud et al. 2006) have a strong rise in their continuum at these wavelengths effectively driving their color blueward with increasing contrast between the AGN and its host-galaxy emission, as evident in Figure 2 with the V_{606}-band distribution (QSOs) in panel *a* shifted higher than that in panel *b*. We note that the rest-frame *U*-band is observed with the V_{606} band for objects with $z \sim 0.7$. Based on these assumptions, color offsets for 81% of our AGN sample are within 0.24 mag. Furthermore, we do not expect our AGNs to reach this value since a significant amount of stellar emission is present in all cases within the small aperture and AGN light is also likely to be emitted at longer wavelengths. We note that if color offsets do reach this level, the contamination is still insufficient to displace AGN hosts from one region to another (e.g., "green valley" to the red sequence). It is more likely that the AGNs contribute an additional ~4% to the total host galaxy flux based on the shift between the median count ratio of the AGN host galaxies and the full galaxy population described above. In § 6 we utilize optical spectra, which are available for 46 AGNs, to further confirm that the AGN host galaxies provide most of the optical light (see Figs. 8 and 9), thus supporting our general conclusions.

3. REST-FRAME COLORS OF MODERATE-LUMINOSITY AGNs

We were motivated by recent studies (Sanchez et al. 2004; Böhm et al. 2006; Nandra et al. 2007) to investigate further the color-magnitude (rest-frame $U - V$ vs. M_V) relation of galaxies hosting moderate-luminosity X-ray-selected AGNs. Since the host galaxies in our sample contribute most of the optical emission, as demonstrated in § 2, we do not need to remove the AGN component from the total (host+AGN) optical emission. We use the rest-frame $U - V$ (i.e., $M_U - M_V$) color up to $z \sim 1$, following Bell et al. (2004) to quantify the color distribution with a greater sensitivity to the continuum slope across the 4000 Å break than is provided by rest-frame $U - B$ color. We note that Wolf et al. (2004) caution that the rest-frame measurement of M_V at $z > 0.7$ is based on an extrapolation of the best-fit galaxy template outside of the observed optical passbands in COMBO-17. For all results presented here, we have confirmed that the same basic conclusions are drawn by using the M_U and M_B rest-frame absolute magnitudes, thus removing the possibility that our results are dependent on the assumed spectral template (i.e., *k*-correction).

In Figure 3*a* we plot the rest-frame colors ($U - V$) as a function of absolute *V*-band magnitude (M_V) for our galaxies, including those hosting AGNs in the redshift interval $0.4 \leq z \leq 1.1$. We confirm past results (Barger et al. 2003; Böhm et al. 2006; Nandra et al. 2007) with better statistics: (1) a high fraction (80%) of moderate-luminosity AGNs reside in the most-luminous ($M_V < -20.7$) galaxies; (2) the rest-frame colors of AGN host galaxies have a broad distribution, over the range $0 < U - V < 1.5$, with no apparent evidence for a color bimodality, as is distinctively evident in the underlying population of galaxies (Bell et al. 2004); and (3) the majority (60%) of AGN host galaxies have bulge-dominated morphologies (Sérsic index $n > 2.5$; Blanton et al. 2003; McIntosh et al. 2005) as marked by small blue dots. Here, we further find that 31%–44% of the AGNs with $M_V < -20.7$ have blue colors, depending on the chosen division ($0.6 < U - V < 0.8$) between blue and red galaxies (Fig. 3*a*, *dashed line*; see Sanchez et al. 2004), thus associating them with star-forming galaxies. This is not surprising since we have a fair number of AGNs at $z > 0.8$, an epoch for which the mean SFR of galaxies has increased by an order of magnitude compared to the present value (e.g., Hopkins & Beacom 2006; Noeske et al. 2007; Zheng et al. 2007). These results are not strongly color biased since both red and blue luminous ($M_V < -20.7$) galaxies, out to $z \sim 1$, mainly fall above the magnitude limits ($R_{ap} \lesssim 24$; Bell et al. 2004) shown by the blue lines in Figure 3*a* ($z = 0.8$, *solid*; $z = 1.0$, *dash-dotted*). We note that some red ($U - V > 1.0$), less-luminous ($-20.7 < M_V < -21.3$) galaxies at $z > 0.9$ may be missed.

It is apparent that the color distribution of these AGNs clearly depends on redshift as shown in Figure 3*b*. Here, we only consider luminous galaxies ($M_V < -20.7$) to minimize any color bias. In

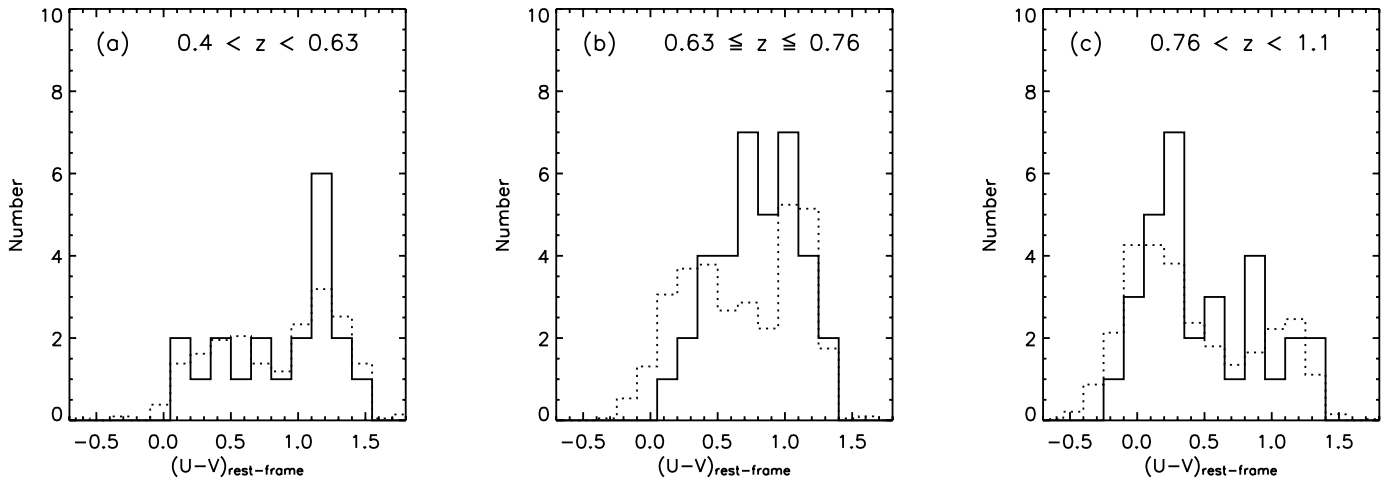

FIG. 4.—Rest-frame color ($U - V$) histogram of galaxies that host AGNs (*solid line*) with absolute magnitude $M_V < -20.7$ in three redshift intervals: (*a*) $0.4 < z < 0.63$, (*b*) $0.63 \leq z \leq 0.76$, and (*c*) $0.76 < z < 1.1$. For comparison, we have plotted, in all panels, the distribution of galaxies (*dotted line*) above this absolute magnitude and renormalized to match the number of AGNs. Note that the peak of the distribution shifts from red to blue with increasing redshift for both galaxies hosting AGNs and the underlying galaxy population.

the redshift interval $0.4 < z < 0.63$ (see Fig. 4*a*), the AGNs tend to have red colors ($U - V > 0.7$) with a mean color $\langle U - V \rangle = 0.86 \pm 0.10$. Within the same redshift interval, the galaxies without AGNs are also preferentially red. We find that 70% (14 of 20) of the AGNs and 62% (239 of 386) of the galaxies have these colors with most associated with the red sequence. In contrast, the mean color of AGN hosts in a higher redshift interval ($0.76 < z < 1.1$; Fig. 4*c*) is $\langle U - V \rangle = 0.49 \pm 0.08$ with 29% (9 of 31) of the AGNs having $U - V > 0.7$. A similar fraction (27%; 211 of 790) of luminous galaxies at these redshifts has these colors. The variance of each color distribution is similar ($s^2 \sim 0.2$). Again, it is as expected that the majority of AGN host galaxies at $z > 0.76$ have blue colors ($U - V < 0.7$) since blue galaxies dominate the luminous population at these redshifts (Wolf et al. 2003; Bell et al. 2004). The null hypothesis, from a Kolmogorov-Smirnov (K-S) test (see Press et al. 1993), has a probability of 2.4% that the distribution of host galaxy colors in Figures 4*a* and 4*c* could be drawn from the same parent population. We have implemented further K-S tests to determine whether the AGN distributions could be drawn from the underlying galaxy population. In Table 1 we give the results that show that the color distribution of AGN host galaxies in Figures 4*a* ($P_{\text{K-S}} = 0.79$) and 4*c* ($P_{\text{K-S}} = 0.21$) resembles that of the overall galaxy population. *We conclude, based on these tests, that the host galaxies of moderate-luminosity AGNs follow a similar passive evolution, or aging, as the underlying galaxy population migrates from blue to red colors with cosmic time.* We note that AGNs with spectroscopic redshifts, shown by small blue dots in Figure 3*b*, confirm this trend.

TABLE 1
STATISTICAL COMPARISON OF COLOR DISTRIBUTIONS

Note	No. of AGNs	No. of Galaxies	K-S (%)	Redshift Range
AGN-Galaxy				
Fig. 4*a*	20	415	79.4	$0.4 < z < 0.63$
Fig. 4*b*	36	669	6.6	$0.63 \leq z \leq 0.76$
Fig. 4*c*	31	957	20.6	$0.76 < z < 1.1$
AGN-AGN				
Fig. 4*a*–Fig. 4*c*	...	...	2.4	...
Fig. 4*a*–Fig. 4*b*	...	...	13.4	...
Fig. 4*b*–Fig. 4*c*	...	...	0.2	...

4. LARGE-SCALE INFLUENCES

As previously mentioned, recent studies (Di Matteo et al. 2005; Croton et al. 2006; Hopkins et al. 2006b) have attributed the truncation of star formation and eventual redward migration of galaxies to merger-induced AGN feedback that effectively populates the red sequence with massive galaxies (Bell et al. 2004; Faber et al. 2006). This scenario may explain the fair number of AGN host galaxies in our sample residing in the "green valley" (see Fig. 3*a*) if they are preferentially located in overdense regions.

In contrast to studies that characterize the environment in terms of density local to AGNs, we are utilizing the fortuitous structures in the E-CDF-S to search for large-scale effects. To do so, we specifically isolate a redshift interval ($0.63 \leq z \leq 0.76$) dominated by two redshift spikes (Fig. 3*b*, vertical dotted lines at $z = 0.67$ and $z = 0.73$, each with $\delta z < 0.02$; Gilli et al. 2003) evident in the 1 Ms CDF-S area, which appear to extend over the larger E-CDF-S area (J. D. Silverman et al. 2008, in preparation). A larger fraction of AGN activity in galaxies within these large-scale structures was reported by Gilli et al. (2003) albeit with limited significance ($2\,\sigma$). Ideally, one would like to consider even narrower redshift intervals ($\delta z \sim 0.02$) to select galaxies cleanly within these spectroscopic redshift spikes, but we are restricted here by photometric redshift errors. Approximately 80% of the galaxies within this redshift interval have errors in redshift (σ_z) less than 0.07,[13] a factor of 2 smaller than the chosen bin width ($\Delta z = 0.14$).

It is evident from Figure 3*b* that the majority of AGNs within this redshift interval have colors ($0.5 < U - V < 1.0$) placing them in the "green valley." Many of the AGNs have spectroscopic redshifts, shown by the small blue dots, that confirm their presence within the narrow redshift spikes ($\Delta z < 0.02$) and their rest-frame colors ($0.5 < U - V < 0.1$; 67%; 12 of 18 AGNs). We plot in Figure 4*b* the $U - V$ color distribution of both AGNs

[13] Photometric redshift errors are based on eq. (5) of Wolf et al. (2004) and a magnitude limit of 23.5.

and galaxies with $M_V < -20.7$ that fall within this redshift interval. We have scaled the galaxy distribution to match the number of AGNs. The color distribution of the host galaxies is clearly different from the underlying galaxy population. *We find that the host galaxies of moderate-luminosity AGNs are preferentially located at intermediate colors* ($U - V \sim 0.8$) *between the red and blue galaxy populations, and skewed toward blue colors*. A K-S test[14] gives a probability of 6.6% that the AGN distribution could be randomly drawn from the underlying galaxy population and suggests that the distribution of these 36 AGNs is different from that of the 669 underlying galaxies.

There does not appear to be any strong selection effects that could be responsible for the color distribution of AGN host galaxies within this redshift interval. Essentially, all of the AGNs have optical luminosities well above the limit at $z = 0.8$ shown in Figure 3*a* by the solid, blue line. By isolating luminous ($M_V < -20.7$) host galaxies, there is clearly no color bias. This is an important point since the 4000 Å break is moving through the *R*-band filter at $z \sim 0.7$ and red galaxies can potentially fall below the flux limit more rapidly than those with bluer colors. There should not be any problems associated with the use of COMBO-17 filters at these redshifts since both rest-frame M_U and M_V fall within the observable window, and multiple filters sample the galaxies' spectral energy distribution below and above the 4000 Å break. Both surface brightness dimming and the use of a fixed photometric aperture can induce systematic changes in color with redshift. An increase in the contrast between a bulge and a disk, due to surface brightness dimming as a function of redshift, would typically redden its rest-frame color; this effect is of most concern when comparing colors over a wider redshift baseline. Bell et al. (2004) address aperture effects associated with COMBO-17 photometry and state that an induced color gradient is only evident at $z \lesssim 0.4$, below the redshift range of our sample, with a potential color offset of ~0.1 mag. There does exists the possibility that the color distribution of AGN hosts is the result of red and blue galaxies having roughly equivalent numbers at $z \sim 0.7$, coupled with our small AGN sample and sensitivity to cumulative biases although our statistical test suggests otherwise.

5. AGN FRACTION

We measure the fraction of galaxies that host AGNs as a function of color and large-scale environment. We follow the technique discussed in § 3.1 of Lehmer et al. (2007) to determine the AGN fraction for our parent population of 5549 galaxies. This method properly accounts for the spatially varying sensitivity limits of the *Chandra* observations of the E-CDF-S (see Fig. 17 of Lehmer et al. 2005). The necessity of this approach is demonstrated in Figure 5, which shows the limiting X-ray luminosity as a function of redshift for the entire galaxy sample and the measured X-ray luminosities of those galaxies harboring AGNs. In addition to the Malmquist bias, there is almost an order-of-magnitude spread in limiting luminosity over the full redshift range. To illustrate these effects, the fraction of galaxies that could host a detectable AGNs with $\log L_X = 41.9$ is ≈23%; this fraction rises steeply to ≈80% when considering a limiting luminosity of 42.5. To account for this selection effect, we determine the contribution of each AGN separately to the total fraction. The AGN fraction (f; see eq. [1] below) and associated error (σ; see eq. [2])

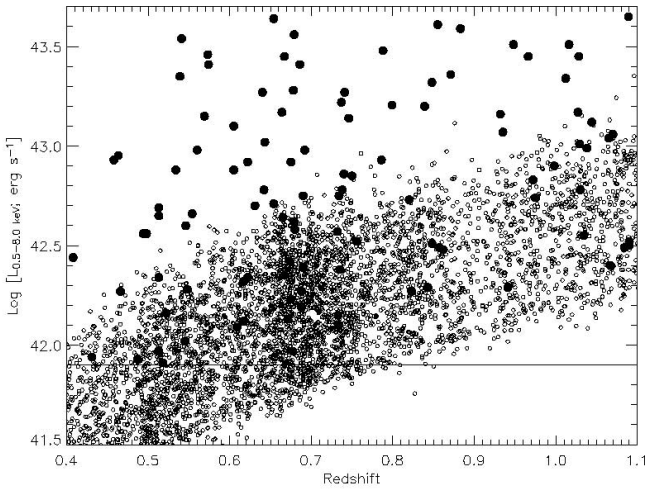

FIG. 5.—Full-band X-ray luminosity as a function of redshift for the 5549 galaxies in our parent sample. The filled circles show the X-ray detections (AGNs); the open circles show upper limits. The spread of a factor of 6 in the value of the limits at a given redshift is produced by the variations in survey sensitivity with location; for a given redshift, the objects with the lowest limits are located at the center of each ACIS pointing and those with the highest limits are located at the edge of the ACIS array. The horizontal line denotes the minimum luminosity for inclusion in our AGN sample.

are a sum over the full sample of AGNs (N) with $N_{\mathrm{gal},i}$ representing the number of galaxies capable of hosting the ith detectable AGNs with X-ray luminosity L_{X}^i:

$$f = \sum_{i=1}^{N} \frac{1}{N_{\mathrm{gal},i}}, \quad (1)$$

$$\sigma^2 \approx \sum_{i=1}^{N} \frac{1}{N_{\mathrm{gal,i}}^2}. \quad (2)$$

We have calculated the fraction of galaxies harboring AGNs in bins of color for the entire sample (Fig. 6*a*). Using a bin width of $\Delta(U - V) = 0.4$, we find that the fraction rises from ~0% at the bluest colors to ~5% at $U - V \sim 0.4$ (i.e., red end of the blue-galaxy population), has a peak in the "green valley" ($U - V \sim 0.8$) with a value of ~10%, and then declines to ~4%–5% at $U - V \sim 1.3$ (i.e., along the red sequence). In Table 2, we list the fraction of luminous ($M_V < -20.7$) galaxies hosting AGN that we measure for various subsamples of galaxies. We note that the AGN fraction in the "field" (i.e., $0.4 \leq z < 0.63$ and $0.76 < z \leq 1.1$) is 5.9% ± 1.0% (51 AGNs from effectively 1157 galaxies) when considering all colors in one bin. Remarkably, the distinct enhancement of the AGN fraction in the "green valley" is due to an overdensity of AGNs in the redshift interval (0.63–0.76) that contains two prominent redshift spikes. In Figure 6*b* we show the fraction of galaxies hosting AGNs in (*solid line*) and out (*dotted line*) of this narrow redshift interval. For an intermediate color interval $0.5 < U - V < 1.0$, the AGN fraction within this narrow redshift range (solid line) is 12.8% ± 2.9% (21 AGNs, 173 galaxies), that reaches ~15% at $U - V \sim 0.8$, while those in the "field" (*dotted line*) have a fraction of 7.8% ± 2.5% (14 AGNs, 246 galaxies). The significance of this higher AGN fraction in large-scale structures is reported here at the 2.6 σ (>99%) confidence level based on the difference and errors of these measurements. This analysis improves on the significance of enhanced AGN activity within large-scale structures previously reported by Gilli et al. (2003). A less conspicuous peak is apparent in the "field" sample

[14] The results of additional tests between the color distributions of AGN hosts (AGN-AGN) in the three redshift intervals are reported in Table 1. We note that their significance is limited given the lack of a large comparison sample that effectively improves the AGN-galaxy comparisons.

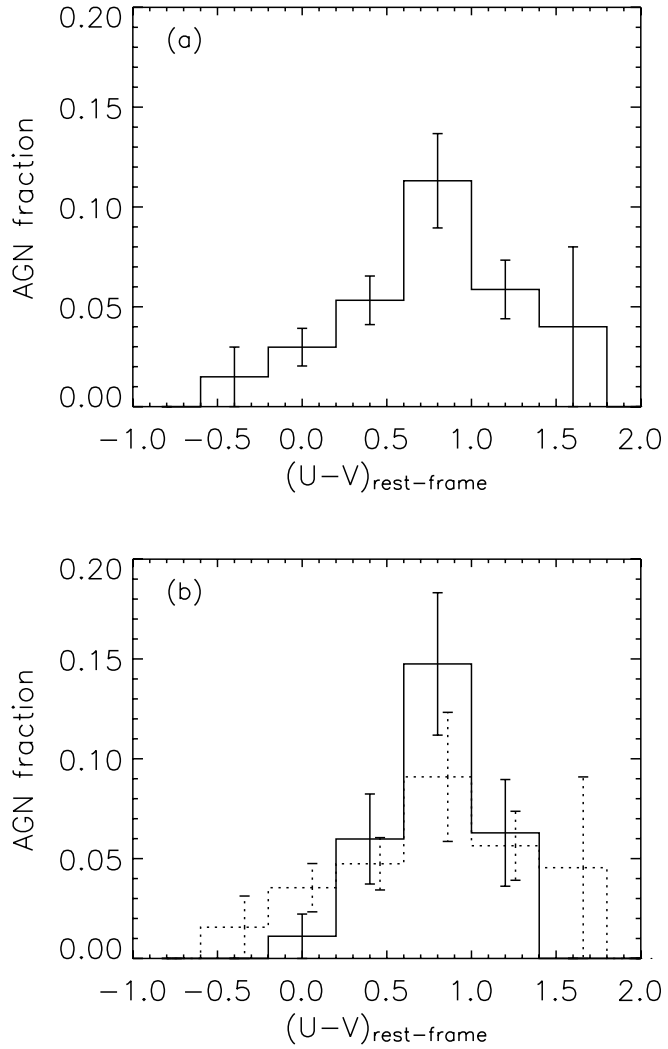

FIG. 6.—Fraction of galaxies ($M_V < -20.7$) hosting AGNs as a function of their rest-frame optical color ($U - V$) for the entire sample (a). In panel *b* we have split the sample into those in (*solid histogram*) and out (*dashed histogram*) of the redshift interval $0.63 \leq z \leq 0.76$. Errors ($1\,\sigma$) are shown for all values with a slight displacement of the dashed set for visual purposes only. A suggestive enhancement ($\sim$2 times, with significance at the $2.6\,\sigma$ level) of AGN activity is evident for host galaxies residing in the "green valley" that is mainly attributed to activity in large-scale structures.

although not sufficiently significant given the current sample size. We find an overall higher AGN fraction in the "field," compared to Nandra et al. (2007) by a factor of $\sim$1.8 although a similar *relative* fraction as a function of color (Fig. 6*b*, *dotted line*); the AGN fraction appears to be rather flat ($\sim$6%) across a wide range of color ($0.3 \lesssim U - V \lesssim 1.5$) that includes the red sequence and the valley but then drops off for blue galaxies beyond the top ($U - V < 0.2$) of the "blue cloud."

6. DISCUSSION

6.1. *Global Evolution of Host-Galaxy Colors*

It is useful to ask what would be the observed color distribution of the hosts of AGNs as a function of redshift up to $z \sim 1$ if we simply assume that AGNs reside in the most luminous galaxies, and hence the most massive, as corroborated by many findings (e.g., Kauffmann et al. 2003; Best et al. 2005). Based on the luminosity function of galaxies from the COMBO-17 (Wolf et al. 2004) and DEEP2 (Faber et al. 2006) surveys, it is evident (Fig. 6 of Faber et al. 2006) that luminous ($M_B < -21$) galaxies at $z \lesssim 0.6$ are predominately red (i.e., early-type). At $z \gtrsim 0.6$, a transition occurs where the majority of luminous galaxies are blue (i.e., late-type, star-forming) as a result of (1) the order-of-magnitude increase in the mean SFR (e.g., Hopkins & Beacom 2006), across all mass scales (e.g., Noeske et al. 2007; Zheng et al. 2007), and (2) strong depletion of galaxies along the red sequence (Bell et al. 2004; Bell et al. 2007) up to $z \sim 1$. In Figure 7 we show the distribution of rest-frame $U - V$ colors for redshift-selected galaxy populations in our sample. The blue peak ($U - V \sim 0$) of the luminous ($M_V < -20.7$) galaxy distribution is most prominent in the highest redshift bin ($z = 0.76$–1.1, *dotted histogram*), while the red peak is more fully populated in the lowest redshift bin ($z = 0.4$–0.63, *dashed histogram*).

We plausibly expect to see a similar redshift dependence in the color distribution of galaxies hosting AGNs with redshift. Observational evidence does exist to support this scenario. Host-galaxy studies, pioneered by *HST*, show that early-type galaxies represent the majority of the hosts of QSOs at low redshifts ($z < 0.3$; e.g., Bahcall et al. 1997). At similar redshifts, Kauffmann et al. (2003) demonstrate that the hosts of over 20,000 narrow-line AGNs from the SDSS are mainly early-type, bulge-dominated systems. The majority of the most luminous, type II QSOs from the SDSS (Zakamska et al. 2006) and radio galaxies (McLure et al. 2004) appear to also have similar early-type hosts. At higher redshifts ($z > 0.5$), there is now evidence that a large fraction of

TABLE 2
FRACTION OF LUMINOUS ($M_V < -20.7$) GALAXIES HOSTING AGNS

Index	Redshift Range[a]	$U - V$ Range	Sérsic Indices	Fraction (%)	Notes
1.....	I+II+III	...	...	6.4 ± 0.8	Full sample
2.....	I+II+III	<0.5	...	4.6 ± 0.9	Blue cloud
3.....	I+II+III	0.5–1.0	...	9.8 ± 1.9	"Green valley"
4.....	I+II+III	>1.0	...	6.0 ± 1.5	Red sequence
5.....	I+III	...	...	5.9 ± 1.0	"Field sample"
6.....	I+III	0.5–1.0	...	7.8 ± 2.5	
7.....	II	0.5–1.0	...	12.8 ± 2.9	Redshift spikes
8.....	I+II+III	...	0–2.5	1.9 ± 0.5	Disks
9.....	I+II+III	...	0–1.5	1.0 ± 0.4	Purely disks
10.....	I+II+III	...	2.5–8	10.6 ± 1.7	Bulges
11.....	I+II+III	<0.7	2.5–8	21.3 ± 5.0	Blue spheroids
12.....	I+II+III	>0.7	2.5–8	7.9 ± 1.7	Red spheroids

[a] I: $z = 0.4$–0.63; II: $z = 0.63$–0.76; III: $z = 0.76$–1.1.

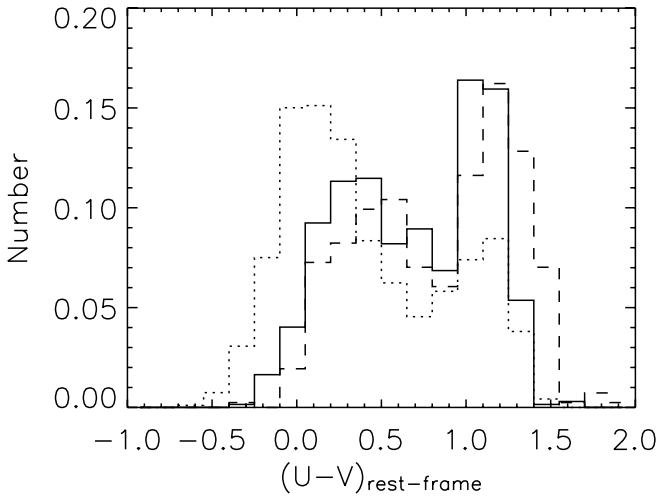

FIG. 7.—Color distribution of all luminous ($M_V < -20.7$) galaxies in three redshift intervals ($z = 0.4$–0.63, *dashed line*; $z = 0.63$–0.76, *solid line*; $z = 0.76$–1.1, *dotted line*). All have been normalized by the number of objects in each interval.

AGN hosts have blue colors and hence significant star formation (Jahnke et al. 2004b; Sanchez et al. 2004; Wisotzki et al. 2006). However, there is little evidence that the host galaxies of AGNs resemble the blue, star-forming galaxies that dominate the galaxy population at $z > 0.8$ as pointed out by Barger et al. (2003) in reference to X-ray-selected samples.

In our sample, the color distribution of luminous ($M_V < -20.7$) AGN host galaxies in the "field" (i.e., outside the redshift interval containing prominent redshift spikes) appears to support the above scenario. In Figure 4 we see that the distribution (*solid histogram*) has both a red (Fig. 4*a*) and a blue (Fig. 4*c*) peak for the $0.4 < z < 0.63$ and $0.76 < z < 1.1$ redshift bins, respectively; these peaks are coincident with those of the underlying galaxy populations (*dotted histogram*). Since the AGN sample is limited in size, this bimodality is only evident when considering AGNs over a wide redshift range and not at each epoch as characteristic of the color distribution of large samples of galaxies (e.g., Strateva et al. 2001; Blanton et al. 2003; Balogh et al. 2004; Baldry et al. 2006; Cassata et al. 2006). The colors of the host galaxies at $z \lesssim 0.6$ are predominately red ($U - V > 0.7$; Fig. 3*b*) and lie on or close to the red sequence. Optical spectra are available for five of the reddest ($U - V > 1.0$) AGN host galaxies and each has a strong 4000 Å break characteristic of an old stellar population. At higher redshifts ($z \gtrsim 0.8$), the AGNs[15] are more prevalent in blue (i.e., star-forming) galaxies. Nine of these high-redshift AGNs with $U - V < 0.4$ have optical spectra that confirm that their colors are dominated by stellar emission. In Figure 8 we show representative optical spectra from our VLT program that are characterized by weak 4000 Å breaks, fairly flat blue continua, and no optical signatures of an embedded AGNs in all but one case (source 333). To summarize, we find that the color distribution of AGN host galaxies has a redshift dependency that reflects that of the underlying luminous galaxy population. It is also apparent that AGNs in the "field" (Fig. 6*b*, *dotted line*) are equally likely to reside in galaxies over a broad range in color with the exception of those at the blue ($U - V < 0.2$) end. This result suggests that AGN activity in the "field" is primarily dependent on mass,[16] given the strong dependency on observed luminosity and weaker in the luminous, blue (i.e., star-forming) galaxy population. In § 6.3 we demonstrate that the lack of an AGN–star formation connection only applies to disk-dominated galaxies.

6.2. *Enhanced AGN Activity in Large-Scale Structures*

The enhancement of galaxies hosting AGNs, in large-scale structures reported in Gilli et al. (2003) and substantiated further in this investigation, appears to indicate the physical scale most nurturing for accretion onto SMBHs. The fraction of galaxies hosting AGNs (Fig. 6*b*) is significantly enhanced within a redshift interval ($0.63 \leq z \leq 0.76$) dominated by two prominent redshift spikes ($z = 0.67$ and $z = 0.73$) that are overpopulated with both AGNs (Gilli et al. 2003) and galaxies (Cimatti et al. 2002; Adami et al. 2005). The dimensions of these structures are estimated to be ~10 Mpc in transverse extent[17] and ~37 ($z = 0.67$) and ~28 ($z = 0.73$) Mpc in depth (R. Gilli 2007, private communication). These two structures have been shown (Gilli et al. 2003; Adami et al. 2005) to be varied in their dynamical state, although both have signs of ongoing collapse (Adami et al. 2005). The "wall" or "sheet" at $z = 0.67$ is described as a loose structure, not yet virialized, and with an embedded compact feature, possibly an infalling group. The $z = 0.73$ "wall" is more compact with a central dense core due to the presence of a cluster (Cimatti et al. 2002; Gilli et al. 2003), and appears to have significant surrounding substructure (Adami et al. 2005) that may eventually collapse into a massive Virgo-type cluster in the local universe. The difference in galaxy populations within these two structures appears to reflect their dynamic state following the well-known SFR-density relation: galaxies in the $z = 0.67$ structure (Fig. 3*b*) are mainly blue, while the $z = 0.73$ structure is dominated by redder (i.e., evolved) galaxies.

Most remarkably, the colors of the host galaxies of these moderate-luminosity AGNs,[18] within the redshift interval $z = 0.63$–0.76, preferentially fall in the "green valley" (Fig. 4*b*). The color distribution is asymmetric, with many hosts closer to the red sequence than the blue galaxy peak. As evident in Figure 3*b*, this color profile is composed of a broad distribution of galaxies residing in the $z = 0.67$ redshift spike and a more compact, red ($U - V \sim 0.8$) group in the $z = 0.73$ redshift spike. It appears that the AGNs follow a SFR-density type relation similar to the galaxies. In Figure 9 we show example optical spectra and *HST* images of four AGNs that have $z = 0.63$–76 and colors placing them in the "green valley." All have no evidence for an embedded AGN (e.g., Hβ or Mg II emission lines) and a relatively mild 4000 Å break. The spectrum of source 85 is characteristic of an E+A galaxy (i.e., poststarburst; Dressler & Gunn 1983; Blake et al. 2004) based on the absorption-line strength (EW = 6.7 Å) of Hδ and weak [O II] emission. E+A galaxies are thought to have undergone a starburst phase ~1 Gyr ago based on the strong contribution from A stars and lack of O and B stars indicative of very recent (~0.01 Gyr) or ongoing star formation. This object is only 1

[15] A handful appear to be associated with a less prominent redshift spike identified by Gilli et al. (2003) at $z \sim 1.04$.

[16] Using eq. [2] of Bell et al. (2005) we confirm that estimates of stellar mass of AGN host galaxies in our sample, based on their rest-frame colors, represent the high end of the galaxy mass distribution since we find a mean of $\sim 1.3 \times 10^{10}\ M_\odot$ and 90% of our sample with $M \gtrsim 3.9 \times 10^9\ M_\odot$, in agreement with optically selected AGN host galaxies (Sanchez et al. 2004).

[17] J. D. Silverman et al. (2008, in preparation) demonstrate that both structures do extend beyond the central 1 Ms region and provide new measures of their angular size.

[18] It is worth noting that Georgakakis et al. (2007) recently reported a color-dependency for AGNs residing in denser environments with rest-frame colors ($U - B \sim 0.8$) coincident with blue galaxies.

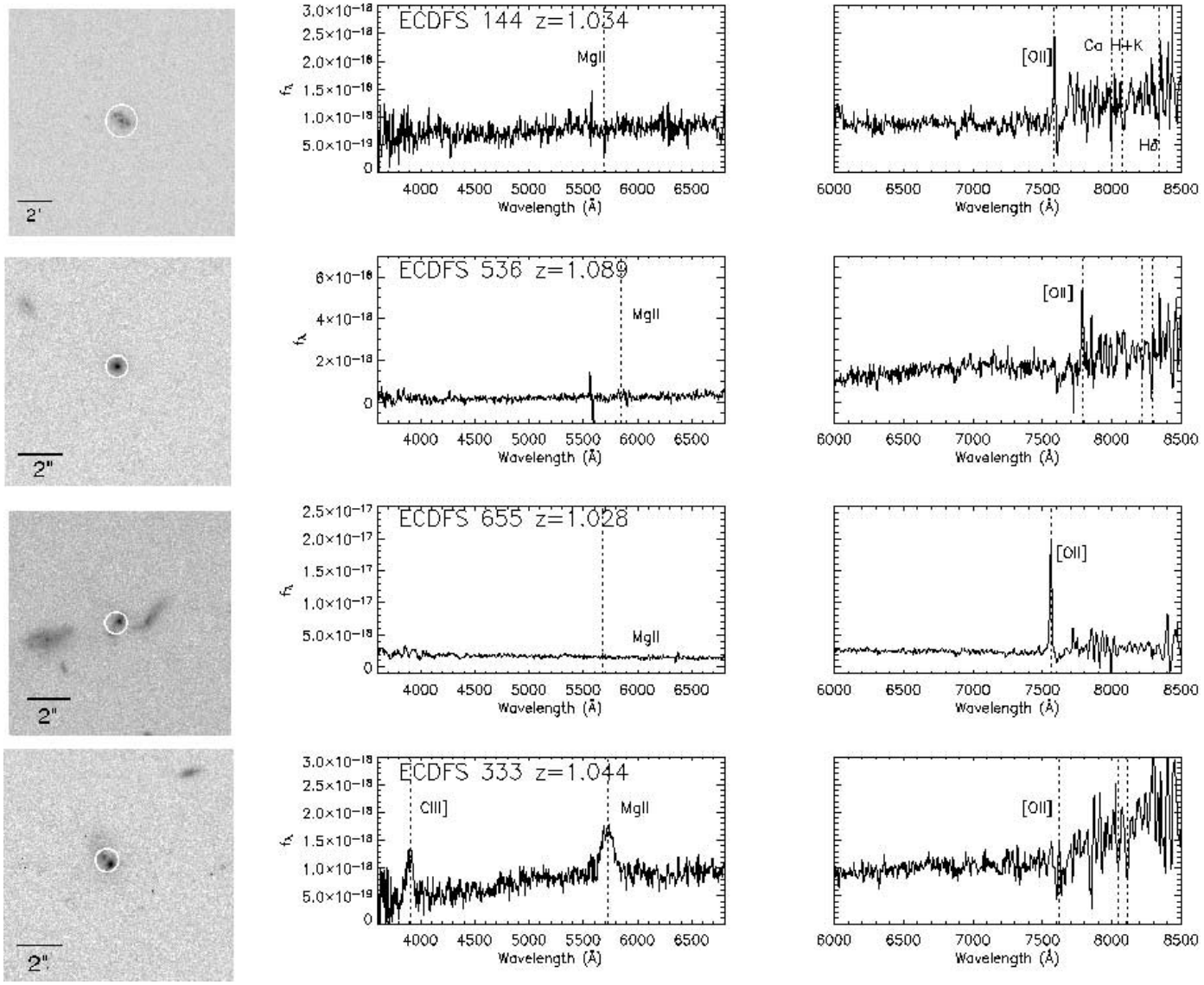

FIG. 8.—Examples of blue ($U - V < 0.4$) galaxies hosting AGNs at $z > 0.8$ that have been identified by our VLT/VIMOS observations. The *HST* ACS z_{850}-band images are shown with a log scaling. The optical spectra that cover a wavelength range of 6000–8500 Å (*right column*) have been binned by 2 pixels. The flux scale is ergs cm^{-2} s^{-1} Å^{-1}. The source numbers follow those presented in the Lehmer et al. (2005) X-ray catalog.

of 15, over the full redshift range, that fall within the "green valley" and has a spectrum characteristic of an E+A galaxy. Therefore, most of these galaxies have not had a major starburst episode within 1–2 Gyr in their past. Most spectra seem to be characteristic of a galaxy, with gradual ongoing star formation, which is best fit by the Type 2 and 3 average galaxy templates shown in Figure 3 of Wolf et al. (2003) effectively separating blue and red galaxies. A larger sample is required to measure statistically the fraction of AGN hosts with poststarburst signatures that have been shown to be common in AGNs from the SDSS (Vanden Berk et al. 2006). *We conclude that within this narrow redshift interval, containing two overdense structures, the enhancement of AGN activity within the "green valley" signifies an important link between the evolution of SMBHs and their host galaxies although not overwhelmingly in poststarburst systems.*

6.3. *Optical Morphology of AGN Hosts*

We highlight the fact that AGN hosts show signs of a bimodal distribution in their colors but not in their morphological properties (Böhm et al. 2006). To illustrate, we have marked those AGNs in Figure 3a that have a radial surface brightness profile (i.e., Sérsic index, n), provided by Häussler et al. (2007) characteristic of a bulge-dominated galaxy ($2.5 < n < 8$). The Sérsic profile of a typical disk-dominated (e.g., late-type) galaxy is that of an exponential function ($n = 1$) while that of a bulge-dominated galaxy (e.g., early-type) is the $r^{1/4}$-law (de Vaucoulers profile; $n = 4$). We find that there are many bulge-dominated galaxies with bluer colors (i.e., ongoing star formation) than a typical red-sequence galaxy and there are a few disk-dominated galaxies that are red. The *HST* ACS images of the red disk-dominated galaxies hosting AGNs show that most (five out of seven with $U - V > 1.1$) of them are highly inclined or edge-on spirals that probably have significant dust extinction. To investigate further, we plot in Figure 10, the Sérsic index versus rest-frame color ($U - V$) for our luminous ($M_V < -20.7$) galaxies and AGNs. We further require here that the science flag provided by Häussler et al. (2007) is 1 for all galaxies that guarantees that GALFIT (Peng et al. 2002) converged; this condition is met for 71 of the 85 luminous host galaxies with morphological parameters given in Häussler et al. (2007). The rest-frame color distribution of this cleaned sample is

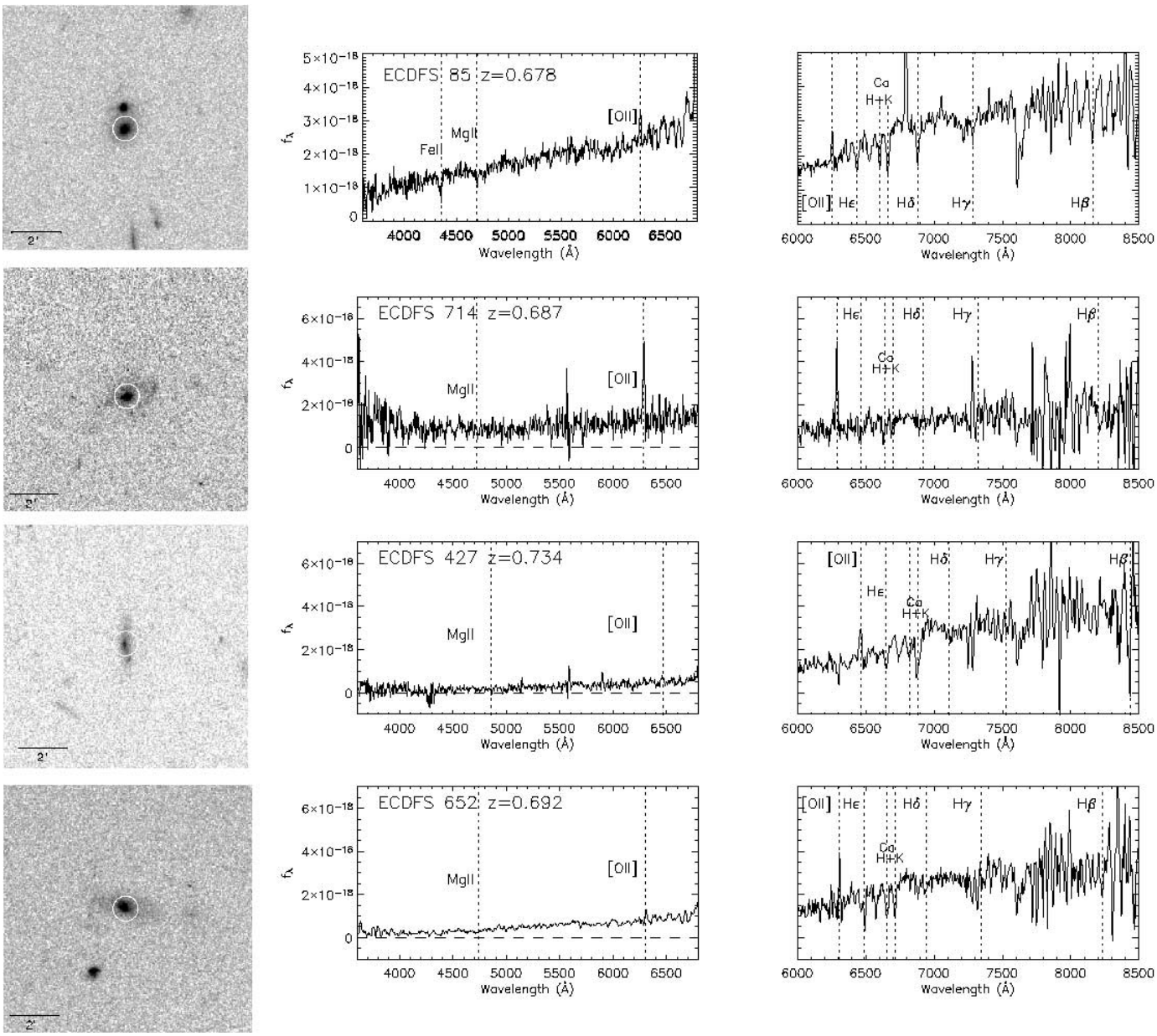

FIG. 9.—Examples of AGN hosts with $0.5 < U - V < 1.0$ and spectroscopic redshifts placing them in the vicinity of the redshift spikes ($z \sim 0.7$). The *HST* ACS V_{606}-band images are shown with a log scaling. Optical spectra are described in the caption of Fig. 8. The source numbers follow those presented in the Lehmer et al. (2005) X-ray catalog.

equivalent to that used in previous analyses since the removed hosts span the full range of color. Symbol types for the AGNs correspond to the three redshift intervals used throughout this work. First, it is evident that the requirement for AGN host galaxies to be bulge-dominated (e.g., Kauffmann et al. 2003) continues up to $z \sim 1$ (Grogin et al. 2005) since 75% have $n > 2.5$ and the fraction[19] of galaxies hosting AGNs as a function of n sharply rises above this value (Fig. 11*a* and Table 2). Second, AGN hosts preferentially become bluer with redshift but retain their bulge-dominated morphology. We conclude that the blue colors of AGN hosts up to $z \sim 1$ are not indicative of star formation in disk-dominated systems.

It is clear that the fraction of bulge-dominated galaxies hosting AGNs is higher for those with blue colors ($U - V < 0.7$); this is shown in the top left quadrant of Figure 10. We measure the AGN fraction (see Table 2), as detailed in § 5, and find that $21.3\% \pm 5.0\%$ of the galaxies with $n > 2.5$ and $U - V < 0.7$ harbor moderate-luminosity AGNs. This is over three times greater than that found for the entire sample irrespective of color or morphology ($6.4\% \pm 0.8\%$; § 5). In contrast, the AGN fraction of purely disk-dominated galaxies ($n < 1.5$) is much lower ($1.0\% \pm 0.4\%$). We conclude that blue, bulge-dominated galaxies have a relatively-high AGN fraction, possibly due to a combination of their massive bulges and gas content.

We further illustrate the color-morphology of our AGN host galaxies by displaying in Figure 12 *HST* ACS color images of six AGN host galaxies in the GOODS area with $n > 2.5$ sorted by rest-frame $U - V$ color. Clearly, the most prominent feature is the bright bulge for all host galaxies. The bluest host galaxy J033213.2−274241, seems to be undergoing a merger. It appears that faint disks may be prevalent in AGNs residing within

[19] The method to determine the AGN fraction (Table 2; index 8-12), using our cleaned sample (science flag = 1), is described in § 5 with n replacing $U - V$.

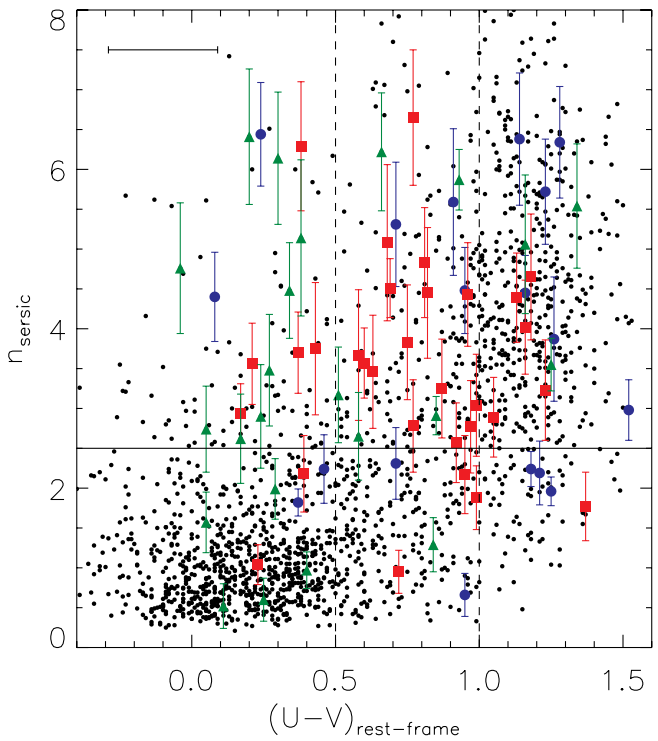

FIG. 10.—Morphology-color relation of luminous ($M_V < -20.7$) galaxies with (*large colored symbols*) and without (*small black dots*) AGNs. The large symbols denote the following redshift ranges: $z = 0.4$–0.63 (*blue circles*), $z = 0.63$–0.76 (*red boxes*), $z = 0.76$–1.1 (*green triangles*). Errors ($1\,\sigma$) associated with n are those reported in Häussler et al. (2007). The bar in the top left corner is the mean $\pm 1\,\sigma$ error on $U - V$ for the AGN host galaxies. The horizontal line divides those galaxies that have either a disk-dominated ($n < 2.5$) or bulge-dominated ($n > 2.5$) morphology as defined in Blanton et al. (2003). The vertical lines highlight the "green valley."

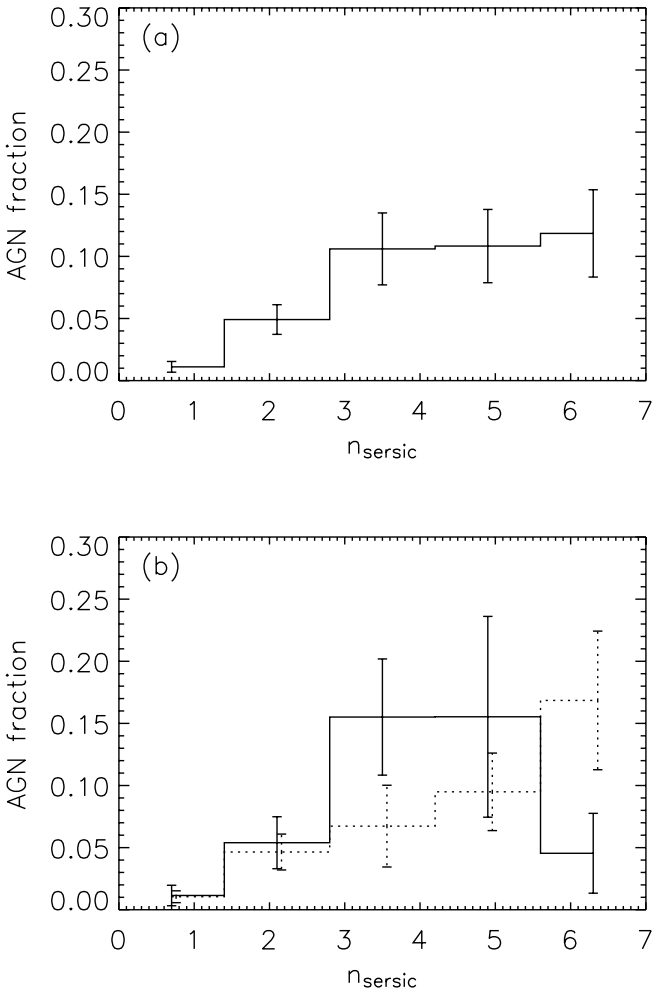

FIG. 11.—Fraction of galaxies ($M_V < -20.7$) hosting AGNs as a function of their morphology (i.e., Sérsic index n) for the entire sample (*a*). In panel *b* we have split the sample into those in (*solid histogram*) and out (*dashed histogram*) of the redshift interval $0.63 \leq z \leq 0.76$ as done in Fig. 6. AGNs clearly reside in bulge-dominated (*panel a*; $n \gtrsim 3$) galaxies with those in large-scale structures (*panel b*; *solid line*) possibly having a higher fraction with faint disks that effectively softens their Sérsic index ($n \sim 3$).

the "green valley"; this is evident in Figure 9 as well. Star-forming substructures may be present in the form of arcs or spiral arms in a few host galaxies (J033226.8−274145, J033246.4−275414). For comparison, the bottom right panel shows a typical red-sequence elliptical galaxy (J033209.7−274248). In Figure 13 we display color images of disk-dominated ($n < 2.5$) AGN host galaxies. Bright, star-forming regions are ubiquitous in the form of knots that appear to lie within spiral arms in most examples.

We remark that a more thorough analysis of the morphological structures of these host galaxies and their relation to the general galaxy population is required and beyond the scope of this paper. We highlight the following complications that are relevant for interpreting these results and will be taken into consideration in a future analysis: (1) Sérsic fits using de Vaucoulers profiles have been shown to have significant uncertainties (e.g., Häussler et al. 2007), (2) the presence of an embedded, optically faint AGNs is likely to affect the measure of structural parameters, such as n, (3) accurate discrimination between bulge and disk-dominated galaxies is difficult since Sérsic indices are known to have significant overlap for these populations (e.g., Sargent et al. 2007), and (4) one must consider redshift-dependent surface brightness effects. A fair number of AGN host galaxies have intermediate Sérsic indices ($1.5 < n < 3$; Fig. 10) and evidence of faint disks as described above. A careful consideration of these issue will enable us to assess the dependence of host-galaxy morphology with environment (Fig. 11*b*). There is suggestive evidence that Sérsic indices of hosts within large-scale structures (Fig. 10, *red squares*) are shifted to lower values ($n \sim 3$). The frequency of bulge-dominated disk galaxies among the hosts of AGNs may be an important test of merger-based evolution models.

6.4. *Are AGNs Driving the Evolution of the General Galaxy Population?*

Numerical simulations (Springel et al. 2005b) demonstrate that accreting SMBHs may be a necessary ingredient in the formation of massive elliptical galaxies from the mergers of gas-rich spiral galaxies. AGN feedback can potentially suppress star formation (Di Matteo et al. 2005) and drive (i.e., accelerate) galaxies onto the red sequence (Croton et al. 2006; Hopkins et al. 2006b). The short timescales (<1 Gyr) for an AGN to provide significant feedback to expel the gas may then instill the color bimodality of galaxies (Springel et al. 2005a) since galaxies with intermediate colors are thought to be evolving rapidly. Strong observational evidence supporting this scenario has been elusive. We now explore whether our AGN sample with well determined host colors and luminosities offers further insight into the AGN-galaxy connection.

The color distribution of AGN host galaxies in our study further substantiates the aforementioned model of galaxy evolution.

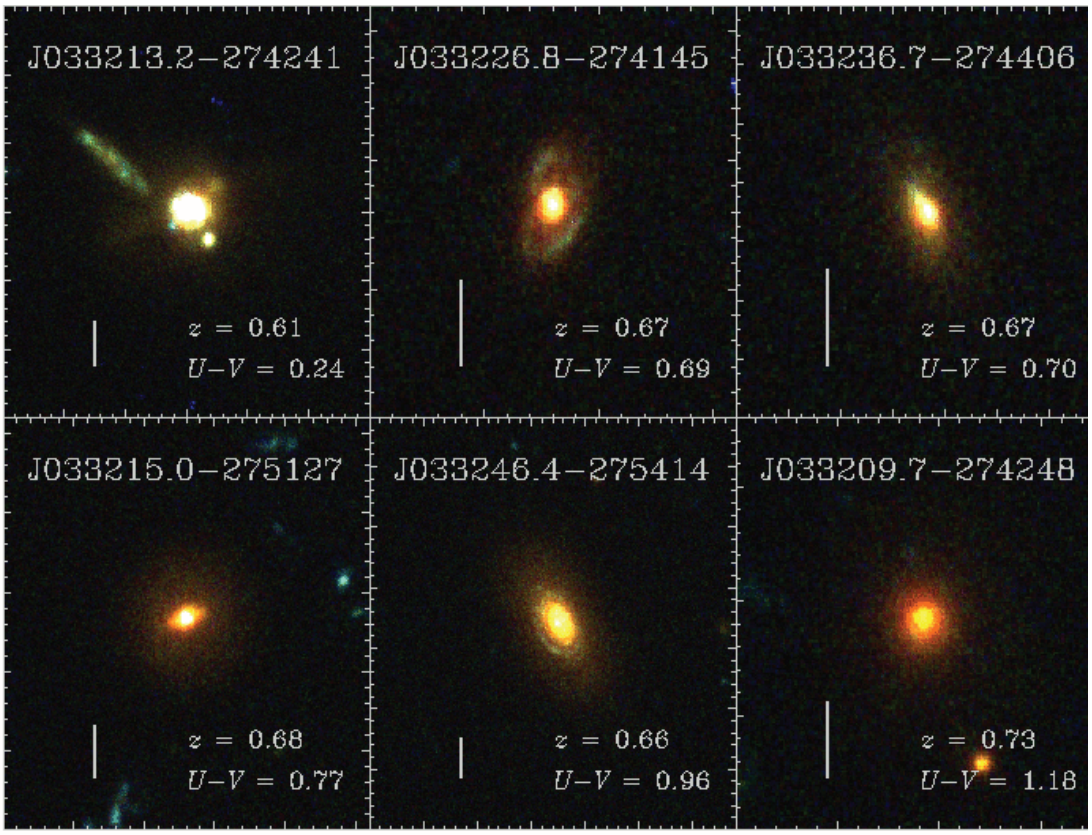

FIG. 12.—Color *HST* ACS postage-stamp images of bulge-dominated ($n > 2.5$) host galaxies located in the GOODS region. Colors correspond to ACS B_{435} (*blue*), V_{606} (*green*), and z_{850} (*red*) bandpass images. In each postage-stamp image, we indicate the source name (*top*), the redshift and rest-frame $U - V$ color of the galaxy (*bottom right*), and a vertical line of length 1.5″ for scaling reference. The images have been sorted by rest-frame $U - V$ color such that the bluest source is located in the top left panel and the reddest source is shown in the bottom right panel.

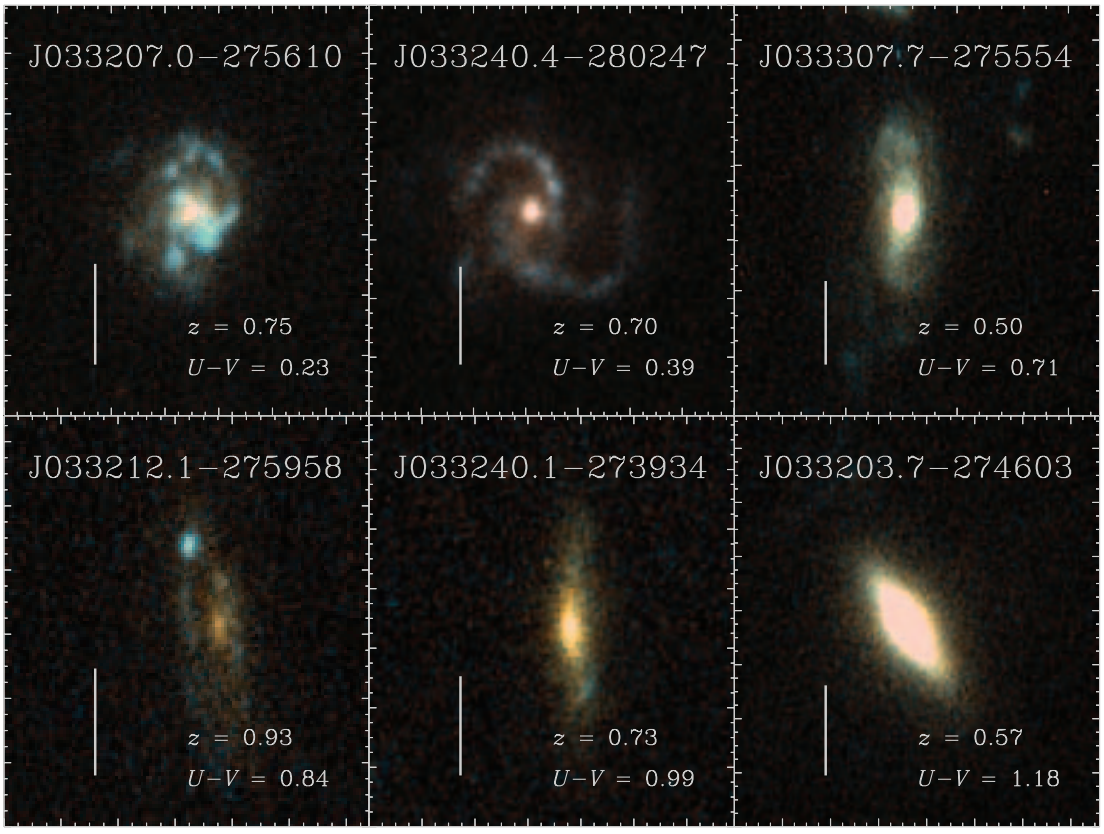

FIG. 13.—Color *HST* ACS postage-stamp images of disk-dominated ($n < 2.5$) host galaxies located in the GEMS area. Colors correspond to ACS V_{606} (*blue*), $(V_{606} + z_{850})/2$ (*green*), and z_{850} (*red*) bandpass images. The labels are described in Fig. 12.

The fraction of galaxies harboring AGNs is significantly enhanced (Fig. 6) in the "green valley," a region on the color-magnitude diagram where galaxies are thought to migrate from blue to red. This higher incidence is associated with galaxies residing in a redshift interval $0.63 \leq z \leq 0.76$ dominated by two large-scale structures that are overdense and have an ongoing assembly of substructure (i.e., galaxy groups and clusters). Within this same redshift interval, the color distribution of the underlying galaxy population (Fig. 7) has rapidly evolved as shown by (1) a significant reduction in the numbers of blue galaxies, a dominant population at higher redshifts ($z > 0.76$), (2) a redward shift of the blue peak, and (3) a dramatic emergence of a red sequence compared to previous epochs ($0.76 < z \leq 1.1$; *dotted line*). This narrow redshift interval ($0.63 \leq z \leq 0.76$), with an elapsed time of 0.73 Gyr, offers a compressed window of the more passive galaxy evolution that occurs over longer timescales of $\sim$5 Gyr ($0.4 < z < 1.1$) as illustrated in Figure 3*b*.

In addition, numerical simulations demonstrate that the color evolution of a merger event slows on approach to the red sequence (Springel et al. 2005a). In Figure 14 we show the color-magnitude relation for galaxies and AGNs within the redshift interval $0.63 \leq z \leq 0.76$ with the evolutionary tracks of mergers, including SMBH feedback, with virial velocity $v_{\rm vir} = 113$, 160, 226, and 320 km s^{-1} overplotted (Springel et al. 2005a). The fact that these models do not account for dust reddening should not severely impact our subsequent findings. Here, we use SDSS photometric bands (u, r) to utilize these models and have converted the photometry to the Vega system. To account roughly for redshift evolution from $z \sim 0.7$ to the present, we have shifted the model magnitude M_r by -1 based on values given for $M_B^\star$ in the literature (see Table 5 of Faber et al. 2006). The evolutionary tracks have ages up to $\sim$5.5 Gyr[20] with the first data point corresponding to 1 Gyr after the initial starburst phase. Based on these model curves, over 1 Gyr has elapsed since the starburst phase concluded for almost all AGN hosts. The majority of AGN hosts cover a broad range of age between 1–4 Gyr and virial velocity between 113 and 226 km s^{-1}. As shown in Figure 14, a large fraction of the merger sequence ($t \approx$ 2–4 Gyr) is spent on approach to the red sequence that should impart an asymmetry in the color distribution of the hosts of AGNs. In Figure 4*b* there may be signs of this since the distribution is skewed with many hosts falling near the blue edge of the red sequence, although a larger sample is required to a make a definitive claim. This effect coupled with our sample size may explain the small numbers of host galaxies with clear poststarburst ($t \lesssim$ 1–2 Gyr) signatures in their optical spectra (Fig. 9). We further speculate that the AGN hosts, situated at the entrance to the red sequence, may either redden with age or further merge with galaxies already on the red sequence (i.e., 'dry mergers'; van Dokkum 2005; Bell et al. 2006) in rich environments that can effectively move them to redder colors and high luminosities/masses since there are few massive ($v_{\rm vir} > 226$ km s^{-1}) and luminous progenitors that could populate the luminous end ($M_r \lesssim -22.5$) of the red sequence. We conclude that the color distribution of AGN hosts further substantiates a coevolution scenario due to mergers and interactions that are effectively nurtured in $\sim$10 Mpc scale structures.

The role of major mergers in triggering AGNs has met observational scrutiny even up to $z \sim 1$, where the merger rate is expected to be higher. Morphological studies (Grogin et al. 2005; Pierce et al. 2007) have yet to find X-ray-selected AGNs at $z >$ 0.5 in such disturbed systems. Here, we confirm the findings of

[20] It is just a coincidence and most likely of no physical significance that these large-scale structures in the CDF-S are present at $z \sim 0.7$, a redshift singled out by Springel et al. (2005a) as a possible formation epoch of elliptical galaxies based an elapsed time of 5.5 Gyr to complete a merger sequence.

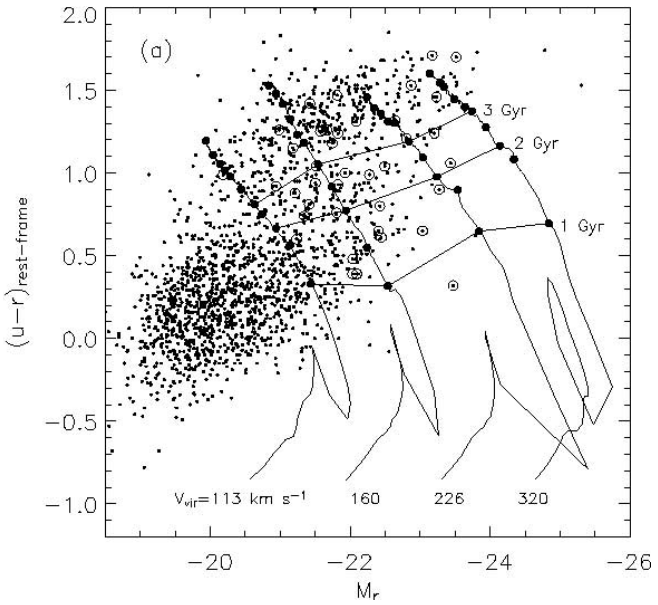

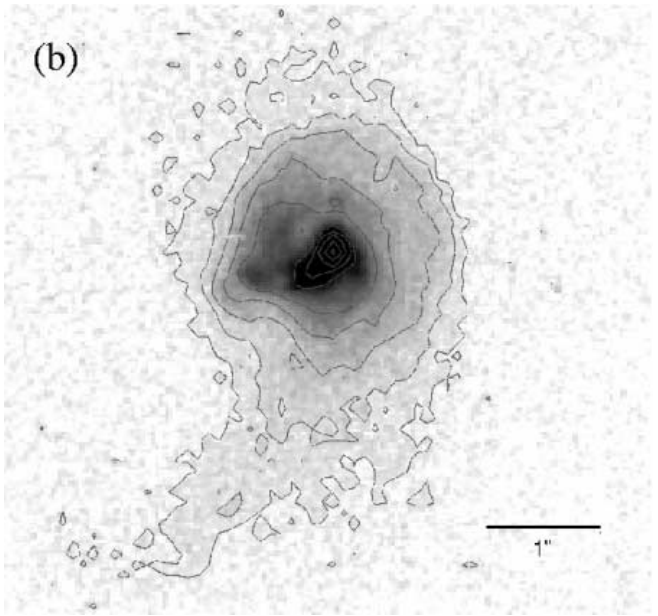

FIG. 14.—(*a*) Color-magnitude relation of galaxies ($0.63 \leq z \leq 0.76$) associated with large-scale structures and AGN-influenced model evolutionary tracks from Springel et al. (2005a). Galaxies hosting AGNs are further marked by an open circle. Theoretical data for merging galaxies is overplotted for galaxies with virial velocities as shown. The large filled circles start from 1 Gyr after the initial starburst phase and each spacing corresponds to 0.5 Gyr. (*b*) *HST* V_{606}-band image of source 66 ($z_{\rm phot} = 0.69$; $L_{\rm X} = 1.5 \times 10^{42}$ ergs s^{-1}) that is the only AGN host galaxy shown above ($M_r = -23.47$; $u - r = 0.32$; $n = 3.56 \pm 0.018$) with a possible merger timescale less than 1 Gyr.

Nandra et al. (2007) that hard (i.e., obscured) AGNs do not populate a distinct region of the color-magnitude diagram as predicted by numerical simulations of merging galaxies that trigger a prequasar (optically hidden) phase (Hopkins et al. 2005). We have further marked those AGNs in Figure 3 with hardness ratios HR $= (H - S)/(H + S)$ indicative of X-ray absorption (HR > -0.2; $\Gamma = 1.9$ with $N_{\rm H} = 10^{22}$ cm^{-2} at $z = 0$). The hardness ratio is a measure of the relative numbers of observed X-ray counts in the soft (S; 0.5–2.0 keV) and hard (H; 2–8 keV) energy bands. We see that hard sources are present over a wide range of rest-frame colors. This is not unexpected since AGNs are known to usually

have parsec-scale molecular tori (Antonucci 1993) with substantial absorbing columns that bear no relation to the presence of star formation. The lack of mergers may reflect the limited sample used to date, since a pair of galaxies undergoing a major merger at $z \sim 0.7$ may only be resolved by *HST* for less than $\sim$1 Gyr of the merger cycle (see Fig. 11 of Springel et al. 2005b). As is evident in Figure 14, the galaxy samples in the E-CDF-S are severely limited for the region on the color-magnitude diagram likely to have merger events between massive ($v_{\rm vir} > 160$ km s^{-1}) galaxies on a timescale of $\sim$1 Gyr after the initial starburst has ended. Three hosts out of our entire sample of 109 AGNs are located on the color-magnitude diagram in a region with $v_{\rm vir} > 160$ km s^{-1} and $\tau < 1$ Gyr, which may be indicative of a major merger. As shown in Figure 14*a*, one of them (source 66) falls within our narrow redshift interval $0.63 \leq z \leq 0.67$ with $M_r = -23.47$ and $u - r = 0.32$. In Figure 14*b* we show the *HST* V_{606}-band image that exemplifies a complex morphology in the nuclear region and tidal features on scales of $\sim$10 kpc ($1'' = 7.1$ kpc at $z = 0.69$) that most likely arise from a major merger of massive galaxies. A second example (J033213.2$-$274241), shown in the top left panel of Figure 12, also shows signs of interaction. We surmise that larger area *HST* surveys of deep extragalactic fields, such as COSMOS (Scoville et al. 2007) with an area coverage of 1.8 deg^2 (5.4 times the area of the E-CDF-S) will provide improved statistics to assess adequately the role of mergers in triggering SMBH accretion.

Finally, we note an alternative to the merger scenario in which galaxies may be more favorable to AGN activity simply due to the presence of a massive bulge and disk that provide the two required ingredients (i.e., a SMBH and a reservoir of gas for accretion; Kauffmann et al. 2007). This is possible since a high fraction ($\sim$21%) of blue spheroids ($n > 2.5$; $U - V < 0.7$) host moderate-luminosity AGNs and there is a slight enhancement of AGN activity in the "field" for galaxies in the "green valley" (Fig. 6*b*, *dotted line*). *HST* images of host galaxies residing within the "green valley" (Fig. 9) appear to have bulges and faint disks. If this were the case, however, we would then not expect such a strong increase in the AGN fraction as a function of environment.

7. SUMMARY

We identified a sample of 109 X-ray-selected AGNs in the E-CDF-S with moderate luminosities ($41.9 \leq \log L_{0.5-8.0\,\rm keV} \leq 43.7$) to investigate the rest-frame colors of their host galaxies. These AGNs have been selected from a parent sample of 5549 galaxies from COMBO-17 and GEMS with $0.4 \leq z \leq 1.1$. Optical spectra are available for 48% of the sample; these provide assurance of the accuracy of the photometric redshifts and show that no strong AGN signatures are present, confirming the stellar nature of their rest-frame colors.

We find that the broad distribution of host-galaxy colors of moderate-luminosity AGNs is due to both (1) the strong color evolution of the underlying luminous ($M_V < -20.7$) and bulge-dominated ($n > 2.5$) galaxy population and (2) an enhancement of AGN activity in large-scale structures. We draw the following three main points:

1. The host galaxies of X-ray-selected AGNs have a color bimodality when excluding a redshift interval $0.63 \leq z \leq 0.76$, which contains two redshift spikes at $z = 0.67$ and $z = 0.73$. Galaxies hosting AGNs at $z \lesssim 0.6$ are preferentially red with many falling along the red sequence. At $z \gtrsim 0.8$, a distinct, blue population of host galaxies is prevalent with colors similar to the star-forming galaxies.

2. The fraction of galaxies hosting AGNs has a prominent peak in the "green valley" that is primarily due to enhanced AGN activity in large-scale structures. Within the redshift interval $0.63 \leq z \leq 0.76$, the AGN fraction reaches a peak value of $\sim$15% at $U - V \sim 0.8$. Over the color interval $0.5 < U - V < 1.0$ we find the AGN fraction to be 12.8% $\pm$ 2.9%, significantly (2.6 σ) higher than that measured in the 'field' (i.e., over all other redshifts; 7.8% $\pm$ 2.5%).

3. We find that AGNs continue to preferentially reside in luminous bulges up to $z \sim 1$. A large fraction (75%) of AGN host galaxies with $M_V < -20.7$ have Sérsic indices $n > 2.5$, even those at $z \sim 1$ that primarily have blue rest-frame colors. Blue, bulge-dominated galaxies ($n > 2.5$, $U - V < 0.7$) are most hospitable for AGN activity based on a measured AGN fraction of 21.3% $\pm$ 5.0% (4 times the fraction of the "field" sample).

The overabundance of AGNs associated with the redshift spikes found in the E-CDF-S and their special location in the color-magnitude relation highlight the importance of environment, on large scales ($\sim$10 Mpc), to influence the evolution of AGNs and their host galaxies. The richness of these structures (i.e., galaxy overdensities, group/clusters in early stages of formation) alludes to mergers as a dominant mechanism to trigger AGN activity, quench star formation and to drive subsequent migration of galaxies from the blue cloud to the red sequence. We compare the color-magnitude relation of our AGN host galaxies with evolutionary tracks of merging galaxies from Springel et al. (2005a) that incorporate AGN feedback. Our AGN host galaxies have colors and morphologies (i.e., bulge-dominated) indicative of evolved systems that had undergone a starburst phase $\approx$1–4 Gyr, and a possible major merger before being observed. These timescales qualitatively agree with optical spectra that do not show overwhelming starburst signatures. These timescales also naturally explain why so few X-ray selected AGN host galaxies appear to be undergoing major mergers. Larger area *HST* imaging surveys such as COSMOS will statistically sample these rare events with timescales less than 1 Gyr.

The E-CDF-S is a unique survey field with a fortunate alignment of large-scale structures for such studies. Our findings exemplify the complexities that must be disentangled to determine underlying relationships between AGNs and their host galaxies. Much optical and near-infrared follow-up is forthcoming in the E-CDF-S that will further our understanding of the connection between coevolution of AGNs and galaxies.

We are especially grateful to the referee for providing insightful comments that strengthened the overall content of this work. We also thank L. Guzzo, K. Iwasawa, A. Merloni, K. Nandra, and I. Strateva for helpful discussions and suggestions. We also recognize the contribution of the GEMS group that provided an early version of their catalog, V. Springel for supplying the model galaxy tracks, and C. Wolf for computing updated photometry. Support for this work was provided by NASA through *Chandra* Award Number G04-5157A (B. D. L., W. N. B., D. P. S.). R. G., C.V., and P. T. acknowledge partial support by the Italian Space agency under the contract ASI–INAF I/023/05/0.

Some of the data presented in this paper were obtained from the Multimission Archive at the Space Telescope Science Institute (MAST). STScI is operated by the Association of Universities for Research in Astronomy, Inc., under NASA contract NAS5-26555. Support for MAST for non-*HST* data is provided by the NASA Office of Space Science via grant NAG5-7584 and by other grants and contracts.

Facilities: VLT(VIMOS)

REFERENCES

Adami, C., et al. 2005, A&A, 443, 805
Alexander, D. M., Smail, I., Bauer, F. E., Chapman, S. C., Blain, A. W., Brandt, W. N., & Ivison, R. J. 2005, Nature, 434, 738
Antonucci, R. 1993, ARA&A, 31, 473
Barger, A. J., et al. 2003, AJ, 126, 632
Bahcall, J. N., Kirhakos, S., & Saxe, D. H. 1997, ApJ, 479, 642
Baldry, I. K., Balogh, M. L., Bower, R., Glazebrook, K., Nichol, R. C., Bamford, S. P., & Budavari, T. 2006, MNRAS, 373, 469
Balogh, M. L., Baldry, I. K., Nichol, R., Miller, C., Bower, R., & Glazebrook, K. 2004, ApJ, 615, L101
Bauer, F. E., Alexander, D. M., Brandt, W. N., Hornschemeier, A. E., Vignali, C., Garmire, G., & Schneider, D. P. 2002, AJ, 124, 2351
Beckwith, S. V. W., et al. 2006, AJ, 132, 1729
Bell, E. F., et al. 2004, ApJ, 608, 752
———. 2005, ApJ, 625, 23
———. 2006, ApJ, 640, 241
———. 2007, ApJ, 663, 834
Best, P. N., Kauffmann, G., Heckman, T. M., Brinchmann, J., Charlot, S., Ivezic, Z., & White, S. D. M. 2006, MNRAS, 362, 25
Böhm, A., Wisotzki, & GEMS Team, 2006, preprint (astro-ph/0612310)
Boyle, B. J., & Terlevich, R. J. 1998, MNRAS, 293, L49
Blake, C., et al. 2004, MNRAS, 355, 713
Blanton, M. R., et al. 2003, ApJ, 594, 186
Brandt, W. N., & Hasinger, G. 2005, ARA&A, 43, 827
Cassata, P., et al. 2007, ApJS, 172, 270
Caldwell, J. A. R., et al. 2008, 174, 136
Cimatti, A., et al. 2002, A&A, 392, 395
Croton, D. J., et al. 2006, MNRAS, 365, 11
Di Matteo, T., Springel, V., & Hernquist, L. 2005, Nature, 433, 604
Dressler, A., & Gunn, J. E. 1983, ApJ, 270, 7
Eastman, J., Martini, P., Sivakoff, G., Kelson, D. D., Mulchaey, J., & Tran, K.-V. 2007, ApJ, 664, L9
Faber, S. M., et al. 2006, ApJ, 665, 256
Ferrarese, L., & Merritt, D. 2000, ApJ, 539, L9
Franceschini, A., Hasinger, G., Miyaji, T., & Malquori, D. 1999, MNRAS, 310, L5
Gavignaud, I., et al. 2006, A&A, 457, 79
Gebhardt, K., et al. 2000, ApJ, 539, L13
Georgakakis, A., et al. 2007, ApJ, 660, L15
Giavalisco, M., et al. 2004, ApJ, 600, L93
Gilli, R., et al. 2003, ApJ, 592, 721
Grogin, N. A., et al. 2005, ApJ, 627, L97
Häussler, B., et al. 2007, ApJS, 172, 615
Hopkins, A. M., & Beacom, J. F. 2006, ApJ, 651, 142
Hopkins, P. F., Somerville, R. S., Hernquist, L., Robertson, B., & Li, Y. 2006a, ApJ, 652, 864
Hopkins, P. F., et al. 2005, ApJ, 630, 705
———. 2006b, ApJS, 163, 1
Jahnke, K., Kuhlbrodt, B., Wisotzki, L. 2004a, MNRAS, 352, 399
Jahnke, K., et al. 2004b, ApJ, 614, 568
Kartaltepe, J. S., et al. 2007, ApJS, 172, 320
Kauffmann, G., et al. 2003, MNRAS, 346, 1055
———. 2004, MNRAS, 353, 713
———. 2007, ApJS, 173, 357
Li, C., Kauffmann, G., Wang, L., White, S. D. M., Heckman, T., & Jing, Y. P. 2006, MNRAS, 373, 457
Lehmer, B. D., et al. 2005, ApJS, 161, 21
———. 2007, ApJ, 657, 681
Le Fevre, O., Vettolani, G., Maccagni, D., & the VVDS Consortium, 2003, Messenger, 111, 18
Le Fevre, O., et al. 2004, A&A, 428, 1043
Martini, P., Kelson, D. D., Kim, E., Mulchaey, J., & Athey, A. 2006, ApJ, 644, 116
Martini, P., Mulchaey, J., & Kelson, D. D. 2007, ApJ, 664, 761
McIntosh, D. H., et al. 2005, ApJ, 632, 191
McLure, R. J., et al. 2004, MNRAS, 351, 347
Merloni, A., Rudnick, G., & Di Matteo, T. 2004, MNRAS, 354, L37
Mignoli, M., et al. 2005, A&A, 437, 883
Miller, C. J., Nichol, R. C., Gomez, P. L., Hopkins, A. M., & Bernardi, M 2003, ApJ, 597, 142
Nandra, K., et al. 2007, ApJ, 660, L11
Noeske, K. G., et al. 2007, ApJ, 660, L43
Peng, C. Y., Ho, L. C., Impey, C. D., & Rix, H.-W. 2002, AJ, 124, 266
Pierce, C., et al. 2007, ApJ, 660, L19
Press, W. H., Teukolsky, S. A., Vetterling, W. T., & Flannery, B. P. 1993, Numerical Recipes in C: The Art of Scientific Computing, 2nd edn.(Cambridge: Cambridge Univ. Press)
Rix, H.-W., et al 2004, ApJS, 152, 163
Rovilos, E., Georgakakis, Georgantopoulos, I., Koekemoer, A., Mobasher, B., & Goudis, C. 2007, A&A, 466, 119
Sanchez, S. F., et al. 2004, ApJ, 614, 586
Sanders, D. B., & Mirabel, I. F. 1996, ARA&A, 34, 749
Sargent, M T., et al. 2007, ApJS, 172, 433
Scoville, N., et al. 2007, ApJS, 172, 38
Silverman, J. D., et al. 2005, ApJ, 618, 123
Springel, V., Di Matteo, T., & Hernquist, L. 2005a, ApJ, 620, L79
———. 2005b, MNRAS, 361, 776
Strateva, I., et al. 2001, AJ, 122, 1861
Sturm, E., et al. 2006, ApJ, 642, 81
Szokoly, G. P., et al. 2004, ApJS, 155, 271
Tremaine, S., et al. 2002, ApJ, 574, 740
Vanden Berk, D. E., et al. 2006, AJ, 131, 84
Vanzella, E., et al. 2005, A&A, 434, 53
———. 2006, A&A, 454, 423
van Dokkum, P. G. 2005, AJ, 130, 2647
Wisotzki, L., Jahnke, K., Sanchez, S. F., & Schramm, M. 2006, NewA Rev., 50, 829
Wolf, C., et al. 2003, A&A, 401, 73
———. 2004, A&A, 421, 913
Zakamska, N., et al. 2006, AJ, 132, 1496
Zheng, X. Z., et al. 2007, ApJ, 661, L41